NAVAL
POSTGRADUATE
SCHOOL

MONTEREY, CALIFORNIA

THESIS

FETCH-LIMITED WIND WAVE GENERATION ON THE CONTINENTAL SHELF

by

Kristen Peta Watts

December 2003

Thesis Advisor: Thomas H. C. Herbers
Second Reader: Edward B. Thornton

Approved for public release; distribution is unlimited

THIS PAGE INTENTIONALLY LEFT BLANK

REPORT DOCUMENTATION PAGE			Form Approved OMB No. 0704-0188
Public reporting burden for this collection of information is estimated to average 1 hour per response, including the time for reviewing instruction, searching existing data sources, gathering and maintaining the data needed, and completing and reviewing the collection of information. Send comments regarding this burden estimate or any other aspect of this collection of information, including suggestions for reducing this burden, to Washington headquarters Services, Directorate for Information Operations and Reports, 1215 Jefferson Davis Highway, Suite 1204, Arlington, VA 22202-4302, and to the Office of Management and Budget, Paperwork Reduction Project (0704-0188) Washington DC 20503.			
1. AGENCY USE ONLY *(Leave blank)*	**2. REPORT DATE** December 2003	**3. REPORT TYPE AND DATES COVERED** Master's Thesis	
4. TITLE AND SUBTITLE: Fetch-Limited Wind Wave Generation on the Continental Shelf			**5. FUNDING NUMBERS**
6. AUTHOR(S) Kristen Peta Watts			
7. PERFORMING ORGANIZATION NAME(S) AND ADDRESS(ES) Naval Postgraduate School Monterey, CA 93943-5000			**8. PERFORMING ORGANIZATION REPORT NUMBER**
9. SPONSORING /MONITORING AGENCY NAME(S) AND ADDRESS(ES) N/A			**10. SPONSORING/MONITORING AGENCY REPORT NUMBER**
11. SUPPLEMENTARY NOTES The views expressed in this thesis are those of the author and do not reflect the official policy or position of the Department of Defense or the U.S. Government.			
12a. DISTRIBUTION / AVAILABILITY STATEMENT Approved for public release; distribution is unlimited.			**12b. DISTRIBUTION CODE**

13. ABSTRACT ***(maximum 200 words)***

The growth of wind waves in coastal areas is limited by the fetch. Understanding this sheltering effect of the coastline on the nearshore wave climate is of critical importance for Navy operations (e.g. amphibious assault and mine countermeasures) in shallow water. Whilst the effect of fetch limitation on the development of the wave field is well understood, the effects of bottom topography, the presence of swell and its interaction with wind waves, the angle of the wind relative to the coastline with regards to the change in effective fetch, and the effects of atmospheric stability, are not well documented. This study investigates fetch-limited wind wave growth by examining cases where a steady wind blows at various angles to a straight coastline, across a continental shelf, in the presence of swell. The observed wind wave growth for offshore winds is consistent with previous observations in the North Sea. The presence of energetic swell opposing the wind does not have a significant effect on the wind sea development. Refraction strongly affects the directional properties of wind waves on the inner shelf. Observed wave growth rates agree well with predictions of the WAVEWATCH III operational wave prediction model forced with COAMPS winds.

14. SUBJECT TERMS Wind Waves, Continental Shelf, Fetch			**15. NUMBER OF PAGES** 93
			16. PRICE CODE
17. SECURITY CLASSIFICATION OF REPORT Unclassified	**18. SECURITY CLASSIFICATION OF THIS PAGE** Unclassified	**19. SECURITY CLASSIFICATION OF ABSTRACT** Unclassified	**20. LIMITATION OF ABSTRACT** UL

NSN 7540-01-280-5500 Standard Form 298 (Rev. 2-89)
Prescribed by ANSI Std. 239-18

THIS PAGE INTENTIONALLY LEFT BLANK

Approved for public release; distribution is unlimited.

FETCH-LIMITED WIND WAVE GENERATION ON THE CONTINENTAL SHELF

Kristen Peta Watts
Lieutenant, Royal Australian Navy
B.Sc., University of New South Wales, 1994
Grad. Dip. Met., Bureau of Meteorology, 1998

Submitted in partial fulfillment of the
requirements for the degree of

MASTER OF SCIENCE IN PHYSICAL OCEANOGRAPHY

from the

NAVAL POSTGRADUATE SCHOOL
December 2003

Author: Kristen Peta Watts

Approved by: Thomas H. C. Herbers
Thesis Advisor

Edward B. Thornton
Second Reader

Mary L. Batteen
Chairman, Department of Oceanography

THIS PAGE INTENTIONALLY LEFT BLANK

ABSTRACT

The growth of wind waves in coastal areas is limited by the fetch. Understanding this sheltering effect of the coastline on the nearshore wave climate is of critical importance for Navy operations (e.g. amphibious assault and mine countermeasures) in shallow water. Whilst the effect of fetch limitation on the development of the wave field is well understood, the effects of bottom topography, the presence of swell and its interaction with wind waves, the angle of the wind relative to the coastline with regards to the change in effective fetch, and the effects of atmospheric stability, are not well documented. This study investigates fetch-limited wind wave growth by examining cases where a steady wind blows at various angles to a straight coastline, across a continental shelf, in the presence of swell. The observed wind wave growth for offshore winds is consistent with previous observations in the North Sea. The presence of energetic swell opposing the wind does not have a significant effect on the wind sea development. Refraction strongly affects the directional properties of wind waves on the inner shelf. Observed wave growth rates agree well with predictions of the WAVEWATCH III operational wave prediction model forced with COAMPS winds.

THIS PAGE INTENTIONALLY LEFT BLANK

TABLE OF CONTENTS

THIS PAGE INTENTIONALLY LEFT BLANK

LIST OF FIGURES

THIS PAGE INTENTIONALLY LEFT BLANK

LIST OF TABLES

THIS PAGE INTENTIONALLY LEFT BLANK

ACKNOWLEDGMENTS

Data for this study was obtained from a variety of sources. I respectfully thank the U.S. Army Corps of Engineers Field Research Facility at Duck, North Carolina, the National Data Buoy Center, the U.S. Navy's Fleet Numerical Meteorology and Oceanography Center, the National Geophysical Data Center, Dr. William O'Reilly (Scripps Institute of Oceanography) and Dr. Fred Dobson (Bedford Institute of Oceanography, Canada) for making these data accessible.

I sincerely thank my advisor, Professor Thomas Herbers, for his expert guidance during this study. His advice, enthusiasm and support were invaluable as well as his wealth of knowledge on travel destinations around the United States. I am very grateful to Professor Edward Thornton for his dry sense of humour, his input and advice as my second reader and for finally remembering my graduation date. My heartfelt thanks also go to Mr Paul Jessen who assisted me enormously with data processing, programming and anything related to computers. His superior MATLAB knowledge saved my sanity on many occasions. Dr Fabrice Ardhuin also receives my gratitude for his expert modelling knowledge and ongoing assistance in setting up and running the WAVEWATCH III model.

To my wonderful family, my dearest friends and my sweetheart, Rai, I thank you for all your encouragement and support from Downunder during my 18 months on the other side of the world. I also thank Mum, Dad, Bryon, Donna, Janette, Wasyl, Katherine and of course, Rai, for enduring the long plane journey to this side of the world and taking care of me whilst I pursue my desire for academic knowledge. I also thank my many international and American friends I met in Monterey, for sharing their culture, and the small, but expanding, Australian NPS community for being my family away from home.

THIS PAGE INTENTIONALLY LEFT BLANK

I. INTRODUCTION

The growth of waves due to energy transfer from the wind has been the subject of numerous studies. Whilst sophisticated theories have been developed for the wind-induced growth and non-linear dynamics of wind waves, very little is known about the dissipation of energy in breaking waves, and therefore the energy balance is not completely understood to this day. As a result, forecasting of wind waves has relied heavily on empirical observations.

For a given wind speed, the growth of wind waves is limited by two variables: the fetch and the duration. The fetch is the distance over which the wind blows over the ocean, and the duration is the time interval of steady wind conditions. In the open ocean where the fetch is unlimited, waves under a steady wind continue to grow until the energy input to the waves equals the energy dissipated. At this stage, the waves have reached their maximum height for a given wind speed and the sea is considered to be fully developed. On the other hand, near a coast with an offshore wind, the fetch is limited and a fully developed sea does not arise. The wind is unable to impart maximum energy to the waves due to this fetch limitation and the wave heights are less than those for a fully developed sea. Duration may further limit wave growth. If a steady offshore wind blows for a sufficient duration, the sea will reach a steady or equilibrium state, in which wave heights increase with distance from shore, to reach full development in the open ocean. Although "ideal" fetch-limited conditions in which a homogenous wind blows perpendicular to a straight coastline, across a deep ocean in the absence of swell, are rare in nature, the topic has been the subject of many studies and has provided valuable insight into the energy balance of wind waves. The object of this study is to further investigate fetch-limited wind wave growth on a depth-limited continental shelf in the presence of swell.

Phillips (1958) recognized that waves cannot continue to grow indefinitely under the influence of the wind, and hypothesized the existence of a saturation or equilibrium range of frequencies over which the energy input and dissipation are balanced and the

waves no longer grow. Using a simple dimensional argument, Phillips proposed a high-frequency equilibrium range:

$$E(f) = \alpha g^2 f^{-5} \tag{1}$$

where g is gravity and α is a numerical constant. This inverse-fifth-power law was shown to be consistent with the observed roll-off of wave spectra above the spectral peak. However, rather than being a universal constant, the value of the parameter α was later found to be variable, dependent on fetch (Hasselmann et al., 1973).

By fitting curves to empirical data, Pierson and Moskowitz (1964) expanded on Phillips' formula by adding to the low frequency end of the spectrum, obtaining a parametric representation for a fully developed wind wave spectrum:

$$E(f) = \alpha g^2 (2\pi)^{-4} f^{-5} \exp\left[-\frac{5}{4}\left(\frac{f}{f_m}\right)^{-4}\right] \tag{2}$$

where the peak frequency, f_m, (corresponding to the maximum of the spectrum) is a function of the wind speed. In this parameterisation, a steep forward face for frequencies less than f_m smoothly matches a high frequency tail with slope of (-5). This widely used parameterisation, called the Pierson-Moskowitz spectrum, became the basis for further developments, which attempted to describe the growth of waves in "ideal" fetch-limited conditions. Kitaigorodskii (1962) proposed a similarity theory in which the evolution of the non-dimensionalised wave energy, β, and peak frequency, Π:

$$\beta = \frac{g^2 E}{U^4} \tag{3}$$

$$\Pi = \frac{f_m U}{g} \tag{4}$$

depend only on the non-dimensional fetch:

$$\chi = \frac{gx}{U^2}. \tag{5}$$

E is the total sea surface variance, U is the wind velocity, and x is the fetch.

A comprehensive investigation of the fetch-limited growth of wind waves was conducted in the well-known Joint North Sea Wave Project (JONSWAP) experiment (Hasselmann et al.) in 1973. The JONSWAP experiment used data from a cross-shore array of wave stations that were located at varying fetches in the North Sea to obtain a parameterisation for the spectral evolution of fetch-limited wind waves. The so-called JONSWAP spectrum essentially adds a peak enhancement function to the Pierson-Moskowitz spectrum:

$$E(f) = \alpha g^2 (2\pi)^{-4} f^{-5} \exp\left[-\frac{5}{4}\left(\frac{f}{f_m}\right)^{-4}\right] \gamma^{\exp\frac{-(f-f_m)^2}{2\sigma^2 f_m^2}} \tag{6}$$

where

$$\sigma = \begin{cases} \sigma_a \text{ for } f \leq f_m \\ \sigma_b \text{ for } f > f_m \end{cases}$$

defines the width of the spectral peak and γ is the ratio of the maximum spectral energy to the maximum of the corresponding Pierson-Moskowitz spectrum. This formulation contains five free spectral parameters. The peak frequency, f_m and Phillips constant, α were scaled according to Kitaigorodskii (1962), and fitted to the JONSWAP observations:

$$f_m = 3.5\chi^{-0.33}$$

$$\alpha = 0.076\chi^{0.22}$$

For the remaining three parameters, constant values were proposed:

$$\gamma = 3.3$$

$$\sigma_a = 0.07$$

$$\sigma_b = 0.09$$

that best fit the JONSWAP observations (Hasselman et al., 1973). The JONSWAP parameterisation was developed under "ideal" wave generation conditions where stationary offshore winds blow over deep water, perpendicular to a straight coastline, in the absence of swell.

The JONSWAP observations confirmed many of the previously known spectral characteristics such as narrow spectral peaks, very steep forward faces and an f^{-5} high frequency tail with a fetch-dependent Phillips constant (Hasselmann et al., 1973). The spectra also exhibited a pronounced overshoot feature, which is illustrated in Figure 1. With increasing fetch, a sharp spectral peak was observed to grow, while shifting towards lower frequency and leaving behind a high frequency tail. Energy at a specific frequency increases to a maximum with increasing fetch and then reduces again as the peak shifts towards the lower end of the spectrum (Komen et al., 1994). Non-linear interactions were proposed as the mechanism by which energy is distributed across the frequencies.

Kahma (1981) studied the growth of the wave spectrum with fetch under conditions that were similar to the JONSWAP experiment except that it was conducted in unstable atmospheric stratification, whereas the JONSWAP conditions were mainly stable. The observed linear increase of the dimensionless energy with increasing dimensionless fetch was similar to that observed in JONSWAP, but with energy levels that were about a factor of two higher at all fetches. Furthermore, the high frequency tail was shown to better fit a (–4) power law as opposed to the (–5) law in the JONSWAP spectrum.

Donelan et al (1985) conducted a comprehensive study of fetch-limited wave growth on Lake Ontario, Canada. Observations were conducted over a wide range of conditions with near-neutral atmospheric stability. Their results supported Kahma's suggestion of a (–4) power law for the high-frequency tail of the spectrum. Donelan et al. proposed a slightly modified JONSWAP spectral model, incorporating a (–4) tail.

There is still considerable debate as to what characteristic velocity, U, should be used in the parameterisation of wind wave spectra. Kitaigorodskii (1983) used U , the wind speed at an altitude no longer affected by the energy and momentum transfer from the atmosphere to the waves, in the derivation of his scaling law. As U is hypothetical, it must be replaced by some measured value of wind speed in practice. The most widely used parameter is the friction velocity, u_*, which is independent of height. However, in the JONSWAP experiment, Hasselmann et al. (1973) argued that the friction velocity is a function of fetch and thus should be considered as an internal variable and proposed

using the wind at 10 m height above the surface, U_{10}, as a more appropriate parameter for scaling. In the present analysis, U_{10} was adopted as the characteristic wind velocity.

Most studies of fetch-limited wave growth concern a steady offshore wind, blowing perpendicular to the shoreline, driving waves travelling predominantly in the wind direction. During the Lake Ontario experiment (Donelan et al., 1985), the effect of the gradient of fetch about the wind direction was investigated for different wind conditions. It was found that when the wind was blowing directly offshore, the direction of the wind and the waves agreed. However, for oblique winds with a large fetch gradient, disparities between the wind and wave direction were as large as 50^0 and it was therefore proposed that the fetch and wind component in the wave direction were more suitable scaling parameters instead of the wind speed and fetch along the wind direction.

Walsh et al. (1989) observed fetch-limited wave growth on the U.S. mid-Atlantic coast using an airborne surface contour radar that provided high-resolution directional wave spectra. Extensive measurements were taken to study slant fetch situations and it was found that this situation produced an asymmetrical directional wave spectrum with a shifted peak. The results from this study were in agreement with the JONSWAP model for wave growth with respect to wave energy and peak frequency (Walsh et al., 1989) and also confirmed the Donelan et al. (1985) relationship for the wave propagation direction in the case of slant fetch situations.

To investigate the effect of water of finite depth on the growth of wind wave spectra, Young et al. (1996) conducted an experiment in a shallow lake of constant depth 2 m. At short fetches, deep-water waves existed and the spectral growth curves were similar to previous studies. However, at longer fetches, the energy and peak frequency became depth limited and a single growth curve no longer existed. Hence they proposed a family of growth curves that depend on the water depth relative to the dominant surface wavelength.

While investigations of idealized fetch-limited conditions have yielded much insight into the wave generation process, natural conditions are usually more complex owing to unsteadiness of the wind, presence of swell, and the coastline geometry and bathymetry, and require a numerical wave prediction model. The WAM model was the

first of today's operational third generation wave models (WAMDI Group, 1988), which integrate the basic energy transport equation from first principles using defined source functions, without any restrictions on the spectral shape. The JONSWAP observations of fetch-limited wave growth were used to calibrate the source terms in the WAM model. The WAM model incorporates finite depth effects and thus can be used as both an open ocean and coastal wave prediction model.

Whilst the WAM model is a vast improvement on previous generation models, it still has some shortcomings. Whereas in the JONSWAP observations, the energy of the wind waves grows linearly with increasing fetch until a fully developed state is reached where the energy remains constant (Komen et al., 1994), in the WAM model, the transition from fetch-limited to a fully developed state is more gradual and the model does not actually achieve equilibrium. Furthermore, the pronounced overshoot of the spectral peak development observed in JONSWAP (Figure 1) is not well reproduced by the WAM model, owing to the crude Discrete Interaction Approximation (DIA) of the non-linear interaction source term. Other operational third generation wave models, such as WAVEWATCH (Tolman, 1991) and SWAN (Booij et al., 1999), are based on a similar formulation and treatment of the source terms as used in WAM model. WAVEWATCH incorporated new refinements in numerical techniques as well as different source terms, while SWAN was designed for specific applications in shallow water. However, the wave growth in these models was calibrated using the JONSWAP observations, and thus wave generation predictions are similar.

Numerous studies have provided further insight into the complex process of fetch-limited wave growth but the effects of the bottom and its topography on the wave growth have been largely neglected. Also, previous experiments have been conducted primarily in protected marginal seas and lakes, in the absence of long period swell. Very little is known about the effect of the presence of swell on wind wave growth. In nature the perfect situation rarely exists and the wave growth is influenced and modified by a number of variable factors – fluctuating winds, irregular coastlines, slant fetches, rough bottom topography, atmospheric stability and the presence of swell. This study further investigates some of these processes and is organised as follows. A description of the various experiments and data sources is given in Chapter II. Chapter III describes the

criteria used for case study selection and the four cases that were chosen for the investigation of fetch-limited wind wave growth. A comparison between the observations from one particular case and wind wave growth relationships from the literature is presented in Chapter IV. In Chapter V the data are compared with COAMPS wind predictions and WAVEWATCH III wave predictions, using various source term formulations. Conclusions are given in Chapter VI.

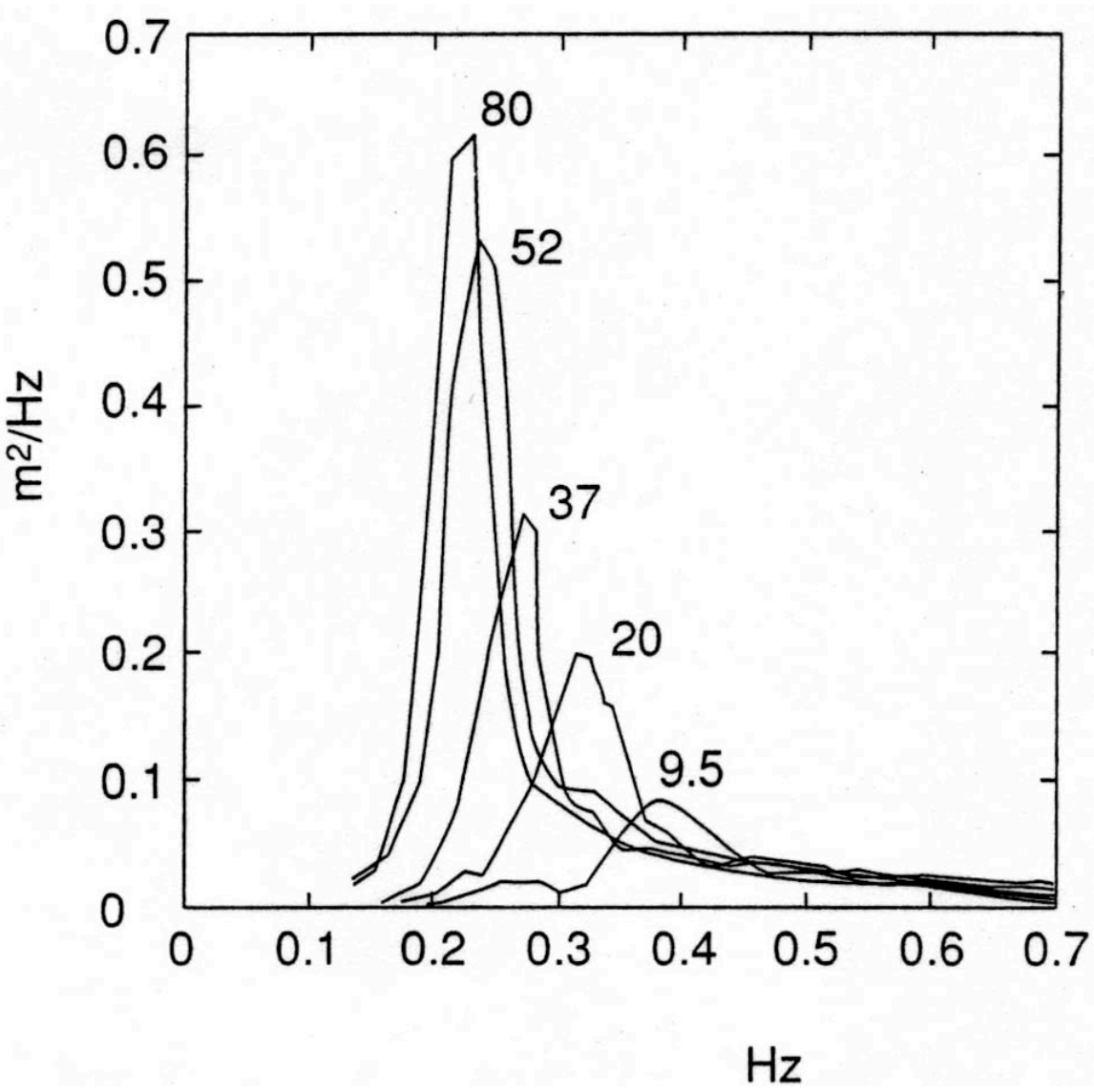

Figure 1. Evolution of wave spectra with fetch for offshore winds. The spectra are labelled with the fetch in kilometres. (from Hasselmann et al., 1973.)

II. DATA AND METHODS

A. FIELD SITE AND EXPERIMENTS

1. Study Area

The datasets used in this study were collected during two separate field experiments, SandyDuck and SHOWEX, which were conducted offshore of the United States Army Corps of Engineers Field Research Facility (FRF) near Duck, North Carolina, in 1997 and 1999 respectively. The instrument sites lie along an east/west transect across the wide continental shelf of the Mid-Atlantic Bight region, midway between Chesapeake Bay and Cape Hatteras, on the United States East Coast. Over this region, the sandy shelf is narrow in the vicinity of Cape Hatteras, widens to approximately 100 km at the study site and continues to broaden to the north near Chesapeake Bay. Water depths at the instrument sites range from 20 – 200 m. The bathymetry is characterised by a gently sloping inner shelf (~1:250), and mid to outer shelf regions with an even gentler slope (1:2500) that are covered with large ridge-like features with horizontal scales of O(5 km) and vertical scales of O(5 m). The offshore shelf-break is oriented approximately north/south while the coastline, a long chain of barrier islands, has a slightly oblique NNW/SSE orientation. In order to define winds with an offshore component for this analysis, the baseline coast was taken to lie along the North Carolina Outer Banks on a line 340/160, from true north.

The prevailing wind direction off the North Carolina coast changes with the seasons. During the summer, southwesterly winds dominate the weather pattern, whilst during winter, the winds are predominantly from the north or northeast. The stretch of coast from Chesapeake Bay to Cape Hatteras is exposed throughout the year to strong winds and rough seas, caused by both tropical and extra-tropical storms. The extra-tropical storm, referred to as the "Nor'easter", can occur at any time of year but the most frequent and intense storms generally develop during November to March. The region off Cape Hatteras, where the Gulf Stream is in close proximity to the coast, is a common place for development or explosive deepening of these storms. The tropical storm, or the hurricane, as it is known in these waters, can also develop in any month but the most likely season is from June to November. Whilst movement of these hurricanes can be

unpredictable and erratic, they generally tend to first move towards the west, then turn northwestward and finally recurve towards the northeast (National Ocean Service, 2002). SHOWEX was marked by the occurrence of four separate hurricanes, including the devastating Hurricane Floyd, and a number of Nor'easter storms. A detailed account of the conditions during SHOWEX is given in Ardhuin et al. (2003). Cold fronts can also rapidly traverse the area from west to east and are more frequent during the winter months. Their passage results in squally southerly winds that quickly shift west or northwesterly as the front passes.

2. SHOWEX

The Office of Naval Research (ONR) Shoaling Waves Experiment (SHOWEX) was conducted from September to December 1999. An array of six Datawell Directional Waverider buoys (X1-X6) was deployed on a cross-shelf transect across the width of the North Carolina continental shelf, on 10-11 September 1999, as shown in Figure 2. Buoy X5 broke loose on 24 October and was subsequently redeployed on 28 October in the same position. Buoy X6 broke loose on 21 September, was later redeployed on 15 October in a slightly different location, and was lost again on 5 December. All other buoys were recovered on 12-13 December 1999 (Table 1).

Buoy	Distance from Shore (km)	Depth (m)	Latitude (North)	Longitude (West)	Dates Deployed
X1	5.4	21	36^0 13.73	75^0 42.28	13 Sep – 13 Dec 99
X2	12.8	24	36^0 13.62	75^0 36.77	11 Sep – 12 Dec 99
X3	22.2	26	36^0 12.27	75^0 29.91	10 Sep – 13 Dec 99
X4	37.7	33	36^0 09.50	75^0 19.53	10 Sep – 13 Dec 99
X5	58.2	39	36^0 07.79	75^0 06.05	13 Sep – 24 Oct 99 28 Oct – 13 Dec 99
X6	86.62 86.57	197 193	36^0 04.98 36^0 04.97	75^0 47.47 74^0 47.50	13 Sep – 21 Sep 99 15 Oct – 5 Dec 99

Table 1. Deployment data for Datawell Directional Waverider buoys during SHOWEX.

The Datawell Directional Waverider buoys are approximately one metre in diameter and are surface following, directional buoys. Wave height spectra and directional wave properties can be calculated from the buoys' measurements of horizontal and vertical orbital displacements, at the sea surface. The buoys sample

continuously for 26 minutes and then internally process the data yielding wave frequency spectra in the range 0.02-0.56 Hz, as well as the mean propagation direction and directional spread as functions of frequency. The resulting spectra, together with the raw time series, are transmitted every 30 minutes to a receiver on shore via an HF radio link. Buoys X5 and X6 were too far from shore for radio transmission, and therefore were equipped with internal data loggers.

3. SandyDuck

Whilst most of the case studies were selected from data collected during SHOWEX, one case from an earlier experiment was also used to complete the range of wind directions for the analysis. The SandyDuck Nearshore Field Experiment was conducted on the inner continental shelf and beach near Duck, North Carolina, from August to November 1997. Extensive measurements of the evolution of frequency-directional wave spectra were collected with a 500 m aperture triangular array of nine sea floor pressure sensors that was deployed 5 km from the shore, in 20 m depth (Figure 3). The spacing of the pressure sensors was chosen to allow for omni-directional wave measurements as well as to accurately resolve sea waves in the frequency range 0.04 Hz – 0.16 Hz. In order to provide measurements of the high frequency portion of the spectrum (0.16 Hz – 0.5 Hz) that is attenuated at the sea floor, a Datawell Directional Waverider Buoy was also deployed within the perimeter of the array.

B. ADDITIONAL WAVE DATA

Permanently deployed wave-measuring instruments, maintained by the U.S. Army Corps of Engineers Field Research Facility, provided additional directional wave measurements in this region. A 15-element coherent array of bottom mounted pressure gauges, located in 8 m depth (8M in Figure 2, see also Figure 3) about 900 m offshore, can resolve frequency-directional spectra up to frequencies of approximately 0.3 Hz. Additional nearshore wave measurements were provided by a Datawell Directional Waverider buoy (WR(FRF) in Figure 2), positioned 4 km offshore in 15 m depth.

The National Data Buoy Center (NDBC) provided additional wave data used in this study (Figures 2 and 4). Approximately 40 km to the south of the SHOWEX array, an infrared laser wave gauge mounted on the Diamond Shoals Lighthouse (DSLN7) C-MAN station, provided wave frequency spectra in the frequency range 0.03 – 0.40 Hz.

Directional wave data was obtained from the NDBC 3-metre discus buoy stations located to the north of the instrument site, at Delaware Bay (44009) and to the east of Virginia Beach (44014). These instruments output wave frequency spectra in the range 0.03 to 0.40 Hz, as well as mean wave direction and directional spread as functions of frequency.

C. WIND DATA

In order to select appropriate fetch-limited conditions for the case studies, historical wind records from six NDBC stations on the North Carolina continental shelf were examined. The locations of these stations are indicated in Table 2 and Figure 4. The continuous winds data archive for each of the instruments provided records of ten-minute averaged wind speed (in m/s) and direction (from which the wind is coming, in degrees clockwise from true north). In some cases, continuous winds data was not available so wind speed and direction were obtained from the NDBC standard meteorological data archive. Here, wind speed and direction were averaged over an eight-minute period for buoys, a two-minute period for land stations and this information was reported hourly. Since wind observations at DUCN7 for November and December 1999 were not available from the NDBC historical archive, the data reported in the FRF meteorological data archive was used instead. These observations of wind speed and direction were vector averaged and reported every 34 minutes.

Station ID	Location	Latitude	Longitude	Station Type	Anemometer Height (above MSL)
44009	Delaware Bay	38.46 N	74.70 W	3m discus buoy	5.0 m
CHLV2	Chesapeake Light	36.91 N	75.71 W	C-MAN station	43.3 m
44014	Virginia Beach	36.58 N	74.84 W	3m discus buoy	5.0 m
DUCN7	Duck Pier	36.18 N	75.75 W	C-MAN station	20.4 m
DSLN7	Diamond Shoals Lt	35.15 N	75.30 W	C-MAN station	46.6 m
CLKN7	Cape Lookout	34.62 N	76.52 W	C-MAN station	14.4 m

Table 2. NDBC permanent wind and wave stations on the North Carolina/Virginia continental shelf. DUCN7 is located within 500m of the FRF 8m array (8M).

To account for the varying heights of the station anemometers above mean sea level, the measured wind speed was converted to a common reference level of ten metres using the log wind profile for statically neutral conditions:

$$u(z) = \frac{u_*}{\kappa} \ln\left(\frac{z}{z_0}\right) \tag{7}$$

where u_* is the friction velocity, $\kappa = 0.4$ is the von Karman constant and $z = 10$ m is the reference level (Stull, 1988). The aerodynamic roughness length, z_0, is obtained from Charnock's relationship for an aerodynamically rough surface:

$$z_0 = \frac{\alpha u_*^2}{g} \tag{8}$$

where $\alpha = 0.0144$ is the Charnock parameter and g=9.81 ms^{-2} is the acceleration due to gravity (Charnock, 1955).

Additionally, winds for a short period were also obtained from a MiniMet meteorological buoy, which was deployed during SHOWEX. The buoy was deployed by Dr. Fred Dobson of Bedford Institute of Oceanography, Canada, at 36^0 10.04 N, 75^0 20.49. W in about 30 m depth (see Figure 2). This instrument recorded hourly observations of standard meteorological data over a one-month period from 18 November to 17 December 1999.

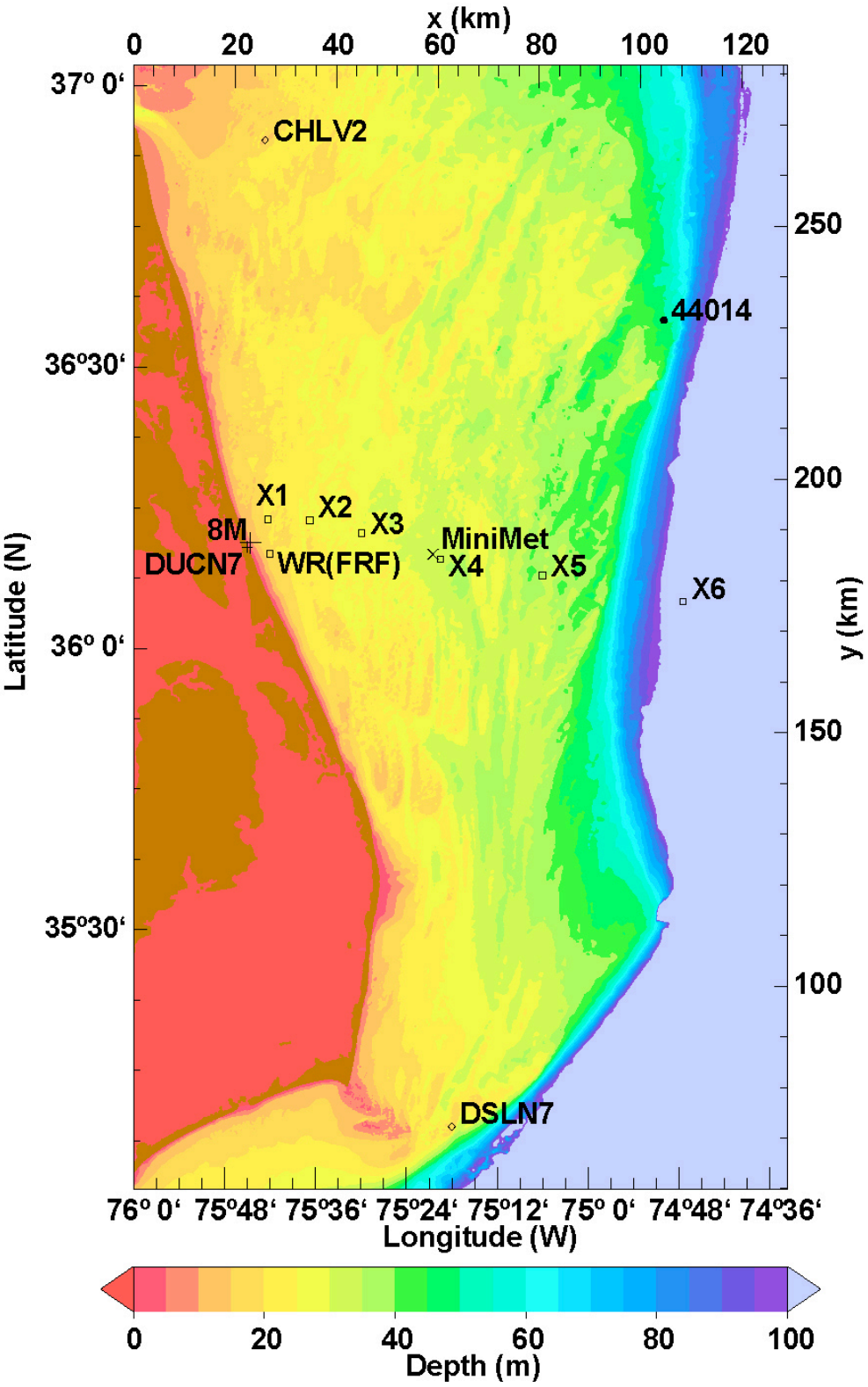

Figure 2. North Carolina/Virginia continental shelf bathymetry with locations of SHOWEX cross-shelf transect and other wind and wave measuring instruments (courtesy of Dr Fabrice Ardhuin).

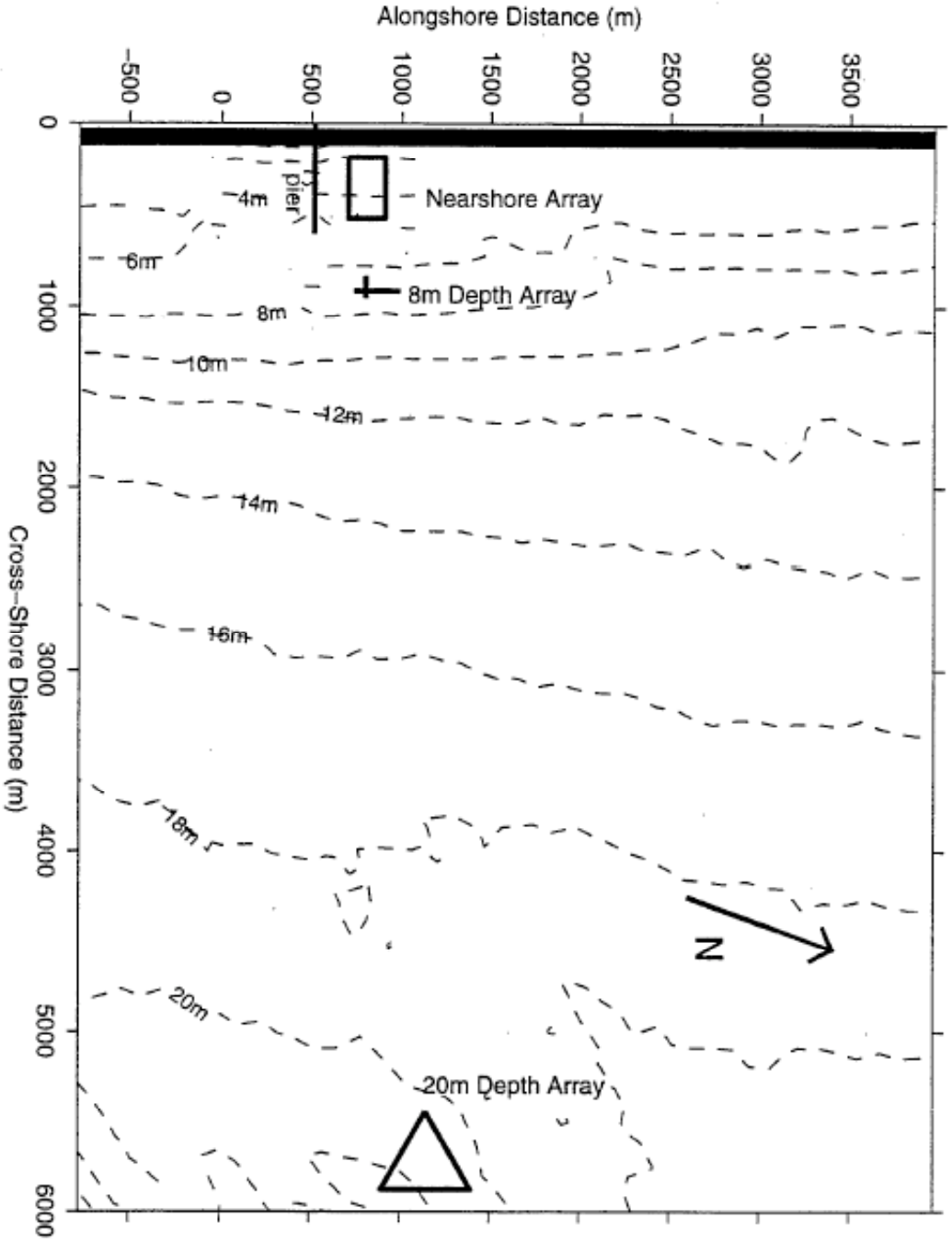

Figure 3. SandyDuck instrument locations (from Borbash, 1998).

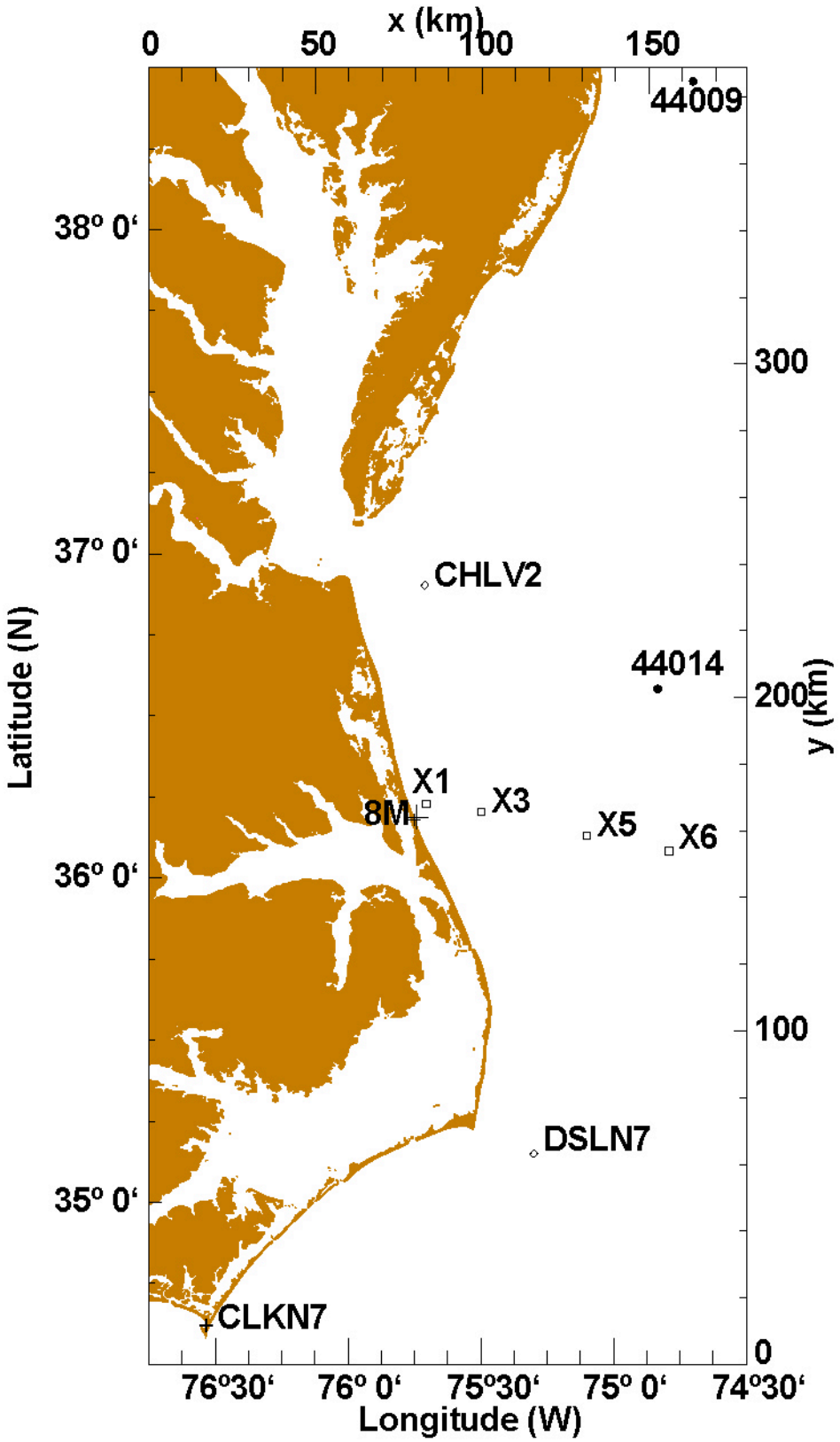

Figure 4. North Carolina/Virginia coastline with locations of NDBC stations and the SHOWEX cross-shelf transect (courtesy of Dr Fabrice Ardhuin).

III. CASE STUDIES

A. SELECTION CRITERIA

In order to select appropriate cases of fetch-limited wind wave growth from the three month long SHOWEX experiment, the wind measurements from the six NDBC stations described in Chapter II were examined. The wind criteria used for case selection are:

- steadiness, in both speed and direction for at least three hours;
- approximately uniform over the study region;
- active wave generation conditions, taken to be wind speeds > 5 m/s; and
- wind directions ranging from offshore to alongshore.

Based on the approximate -20^0 N orientation of the coastline, winds with directions from 160^0 clockwise to 340^0(from true north) were considered to have an offshore component.

Winds for the NDBC station at the Duck Pier (DUCN7) for the entire SHOWEX period are shown in Figures 5 and 6. The horizontal lines in these figures bracket the range of wind directions with an offshore component that correspond to fetch-limited conditions. The observations include numerous offshore wind events. However, offshore wind conditions that typically occur during the passage of fronts, storms and hurricanes are usually highly variable with a rapidly veering wind direction. There were only a few time periods during SHOWEX with sufficiently steady offshore or alongshore winds, for the purposes of this study. These cases were chosen somewhat subjectively, using the above criteria and examining the winds from all the NDBC stations in further detail.

Once suitable wind criteria were met, the wave frequency and directional spectra for each case were examined in order to ensure that the wave field was also steady over the selected time period. Each case was then narrowed down to a three hour time period for further investigation into the wave growth with increasing fetch.

B. CASES SELECTED

1. SHOWEX (1999)

Three time periods during SHOWEX were selected for analysis of fetch-limited wind wave growth. The details are given in Table 3. The direction of the winds varies from almost northerly winds for Case 1, to alongshore north-northwesterly winds for Case 2 and approximately offshore westerly winds for Case 3.

Case	Date	Time	Average Wind Direction	Average Wind Speed (m/s)	Remarks
1	5 Oct 99	1800-2100	352	9.4	N'ly Winds
2	1 Dec 99	0600-0900	343	14.0	Alongshore NNW'ly Winds
3	3 Nov 99	1330-1630	272	9.3	Offshore W'ly Winds

Table 3. SHOWEX cases chosen for analysis.

Whilst these three cases span a range of different wind directions, they all lie in the same quadrant having only northerly or westerly components. Suitable cases, which fit the selection criteria but had offshore winds from a southerly direction, were not found in the three months of SHOWEX data.

2. SandyDuck (1997)

In order to obtain a broader range of offshore wind cases for analysis, an additional case (Table 4) was selected from the SandyDuck field experiment, which took place two years earlier in the same geographic location. Figure 7 shows the winds from four NDBC stations for the selected twelve-hour time period.

Case	Date	Time	Average Wind Direction	Average Wind Speed (m/s)	Remarks
4	17 Aug 97	2200-0100	224	9.2	Offshore SW'ly Winds

Table 4. SandyDuck case chosen for analysis.

Although the wind direction in this case is remarkably steady across the shelf for the entire twelve-hour period, the wind speed varies spatially and temporally over the study area with strong winds (up to 15 m/s) at Diamond Shoals located 100 km south of the

SandyDuck experiment site. This case is more complex than the others owing to these large spatial variations in wind speed and illustrates, as explained below, non-local effects on fetch-limited wave generation.

C. CASE ANALYSIS

1. Case I – 5 October 1999

The wind observations from each of the NDBC stations for Case 1 are shown in Figure 8. This case exhibits a relatively steady, northerly wind, whose direction is marginally outside the range of fetch-limited conditions. This alongshore wind has a slight onshore component and subsequently the fetch is close to infinite for most of the continental shelf. Fetch limitations are expected only at the nearshore buoys and array where the wave propagation paths are affected by refraction over shallow bathymetry.

Energy spectra, mean wave direction and directional spread, versus frequency, averaged over a three hour period (Figure 8), are shown in Figures 9 and 10, the former showing the inner shelf instruments whilst the latter shows the outer buoys in the SHOWEX transect. The mean wind direction, obtained by averaging the wind directions from the four NDBC stations closest to the transect (CHLV2, DSLN7, 44014 and DUCN7) over the three hour time period, is indicated by the horizontal dashed line in the mean direction panel. Data from X6 is unavailable for this case study, as this buoy broke loose on 21 September and was out of service until 15 October.

The energy density spectra show a broad maximum in energy with no clear separation between the wind wave and swell peaks. Energy levels at the peak frequency increase only slightly with increasing distance from shore with the exception of significantly higher levels observed at buoy X5. As X5 is situated near the shelf break and waves from the north would have to travel over the shallow continental shelf before reaching this buoy, this increase in energy level is most likely caused by local refraction effects. At frequencies above the peak, the spectra from all instruments collapse on top of each other. The relatively small variations between observed wave spectra suggests that fully developed conditions persisted across the shelf. Only at the shallowest instruments, (WRFRF and 8M) a reduction in wind sea energy levels is noted that may be the result of refraction and coastal sheltering effects. The significant variability at all buoys at the

lowest frequencies is considered to be noise, caused by inaccuracies in the buoy response. As the energy level in this region of the spectrum is so low, measurements of directional properties are not expected to be reliable.

The mean wave directions exhibit a similar pattern at all sites except for the closest inshore instrument (8M array) and the furthest offshore buoy (X5). As the wind direction is nearly parallel to the depth contours, the predominantly alongshore-propagating wind wave energy will be affected by refraction over the shallow bathymetry inshore, and propagate along curved trajectories towards the coast. This refraction effect can be seen in the observed mean directions at low frequencies (Figure 9), which are at a significant angle to the wind. At the shallowest 8M array site, the mean wave direction deviates by about 20^0 from all other locations. Here refraction is felt across a wider range of frequencies causing direction shifts as large as 90^0. At high frequencies, the mean wave direction tends towards the mean wind direction for all of the instruments except buoy X5. A possible explanation for this difference is that the winds observed at the offshore 44014 and 44009 stations were consistently blowing at about a 20^0 angle relative to the winds measured further inshore (Figure 8).

The directional spreading estimates indicate that the wave spectra are narrowest in the vicinity of the spectral peak and broader at both higher and lower frequencies, consistent with previous observations (e.g., Young and Verhagen, 1995). The 8M array shows significantly less directional spread at low frequencies than the other instruments, possibly owing to severe refraction in very shallow water close to the coast. In addition to refraction, limited fetch for offshore propagating waves may also affect the directional properties close to shore. As the mean wind direction is slightly onshore, waves generated in the wind direction, or on the offshore side of this direction, will experience an unlimited fetch and therefore grow to full development. On the other hand, waves generated on the inshore side of the mean wind direction will be severely fetch-limited due to the presence of the coast, and this will result in reduced growth. This asymmetrical fetch effect is most noticeable at the 8M array, which is only about 900 m from the coast. Waves arrive at this instrument only from offshore as the extreme fetch limitation on the coastal side will limit wave generation in that region, resulting in a reduced directional spread. This sheltering effect may also contribute, in addition to

refraction, to the reduced energy levels noted at the 8M array and to a lesser extent, at the WRFRF buoy.

Figure 11 shows the two-dimensional energy density spectrum (averaged over the same three-hour interval) for four locations, spanning the shelf from the shallow 8M array to buoy X5 offshore. The spectra are similar across the transect exhibiting a broad uni-modal peak that is slanted towards normal incidence (70^0) at low frequencies. This peak bifurcates into a bimodal structure at high frequencies, with two peaks distributed approximately symmetrically on either side of the mean wind direction. This transition to a bimodal spectrum at high frequencies has been noted in a number of earlier studies (eg. Young & Verhagen, 1995 and Wang & Hwang, 2001) and is considered to be a robust feature of fetch-limited wind wave spectra. The cause of this bimodality is believed to be nonlinear interactions that transfer energy from the dominant waves that travel in the wind direction to obliquely propagating waves at higher and lower frequencies (for further discussion, see Young and Verhagen, 1995).

2. Case II – 1 December 1999

The NDBC station wind observations for Case II, as well as the winds from the MiniMet buoy, which was operational during this period, are shown in Figure 12. The mean winds in this case are strong, steady north-northwesterlies. The direction differs by only about 10^0 from that in Case I but the winds are slightly stronger and more alongshore, further restricting the fetch at the inshore stations. The winds are generally uniform in direction across the instrument transect, but there is some spatial variability in the wind speed. Comparisons of the observed winds at DUCN7, the MiniMet buoy (which is in the vicinity of X4), and 44014, indicate a gradual increase across the shelf from about 10–12 m/s near the coast to 15–18 m/s at the shelf break.

Figures 13 and 14 show the energy spectrum, mean wave direction and directional spread. The spectra are generally similar at high frequencies whereas the spectral peak level increases across the outer shelf between buoys X2 and X6. This is likely the result of the gradual increase in wind speed across the shelf, as opposed to a coastal effect. Evidence of coastal sheltering effects is noted at intermediate frequencies (0.15 – 0.35 Hz) on the inner shelf. In this range, the spectra for the offshore instruments (Figure 14)

collapse, but at the inner shelf instruments (Figure 13), there is a systematic decrease in energy levels towards the shore. These variations on the inner shelf are likely caused by the effects of refraction and asymmetric fetch, both of which tend to reduce energy levels and shift the mean wave direction towards onshore propagation, as discussed for Case I.

The effects of asymmetric fetch are more dramatic in the mean wave direction and directional spreading estimates for the inner shelf instruments in Case II than for Case I. For Case II, the mean wind direction is almost alongshore, causing the fetches on the shore side of the wind to be even more significantly reduced than that for Case I, where the wind was directed slightly onshore. This is particularly evident at intermediate frequencies at the 8M array. Whereas in Case I, the mean direction differs from the other instruments by about $10\text{-}20^0$, here the differences are as large as 40^0 at 0.3 Hz. The directional spread at this array is also significantly less than that for the other instruments.

The systematic large shift in the mean wave direction away from the wind at lower frequencies, particularly evident at the inner shelf instruments (Figure 13), is caused primarily by refraction. Low frequency waves travelling at large oblique angles to the coast, are strongly refracted over the sloping bottom and turn towards the coast. At the lowest frequencies, waves are travelling almost normal to the wind direction. As the wind forcing is expected to be weak at this large angle, the effect can only be explained by refraction.

Figure 15 shows the two-dimensional spectra for Case II at four locations across the SHOWEX transect. The effect of refraction across the shelf is noticeable at all buoys in the form of a slanting ridge of energy. In particular at the 8M array and at X1, the maximum energy is concentrated around the onshore direction, (~070) nearly perpendicular to the wind direction. Similar to Case I, the spectra show a transition from a unimodal spectrum at low frequencies to a bimodal spectrum at high frequencies. However, in this case, the two peaks are not symmetrically distributed about the mean wind direction, but one of the peaks is aligned with the wind direction. Wang and Hwang (2001) noted that when the local wind direction and the mean wave direction were not closely aligned, an asymmetry in the bimodal distribution resulted. In this case there is indeed considerable directional shear in the energetic part of the spectrum (Figure 15).

The nonlinear interactions involving lower frequency swell components travelling at a large angle to the dominant wind waves, may contribute to the asymmetry of the spectrum at high frequencies.

The differences between the spectra for Cases I and II indicate that the evolution of the wave spectrum is sensitive to the orientation of the wind with regards to the coastline. There is only a 10^0 difference between the mean wind directions of these two cases, but in Case II the inner shelf is sheltered by the coast, owing to the combined effects of restricted fetch and refraction.

3. Case III – 3 November 999

Case III, with an offshore wind, features more severe fetch-limitations and refraction effects than the previous two cases. The wind observations at all NDBC stations (Figure 16) show a westerly wind that is relatively steady in direction, but with some variability (±28% about the mean) in speed, both spatially and temporally. The average wind speed over the three-hour case time is about 9.3 m/s. Winds to the north, at 44009, are somewhat stronger but this does not significantly affect the generation of waves by offshore winds at the instrument transect.

The energy density spectra (Figures 17, 18) are bimodal with clearly separated wind sea and swell peaks. The wind sea peaks exhibit the classic fetch-limited shape with very steep forward faces, a high frequency tail evolving with increasing fetch with pronounced overshoot of the peak levels. In this case, the mean wind direction (~270^0) is close to perpendicular to the coastline (orientated 340/160), resulting in limited fetches for all wave generation directions. However the small 20^0 angle to shore normal is significant, causing asymmetric fetches for directions oblique to the mean wind direction. Waves arriving from south-westerly angles will have a shorter fetch than those arriving from north-westerly directions. As a result, maximum wave energy is generated in a direction shifted slightly to the north of the wind direction. These offshore propagating waves travel at an angle to the bathymetry contours and thus will undergo refraction. Due to the orientation of the mean wind direction and the coastline, waves will tend to be refracted towards the south.

The combined effects of asymmetrical fetch and refraction are evident from the mean wave directions, particularly at the inner shelf instrument locations (Figure 17). At high frequencies, waves at all locations travel approximately in the wind direction but at intermediate frequencies, the asymmetrical fetch effect becomes apparent and at lower frequencies, waves interact with the bottom and are strongly refracted towards the shoreline. For example, at the WRFRF location (15 m depth), 0.4 Hz waves are in deep water, so the shoaling bottom will have no influence on ray paths. The waves however are observed to begin shifting from the mean wind direction towards the south at this frequency and hence the effect of asymmetric fetch, which causes more wave generation at longer fetches, must be influencing wave propagation at this location and frequency. Below 0.3 Hz, waves are travelling almost normal to the mean wind direction. The wind cannot drive waves at this large an angle. At this frequency, waves are transitioning from deep to shallow water and begin to be influenced by the bottom and refracted towards the coast.

Figure 19 shows the two-dimensional energy density spectra for four instruments across the shelf. Two distinct energy peaks are evident for buoys X1, X3 and X6, which indicate a clear separation of the low frequency swell and the wind generated sea. The effects of refraction are apparent in the dramatic shift in direction at the intermediate frequencies (0.15 – 0.35 Hz), in particular at buoy X1. Here the dominant wave direction varies by about 120^0 from the mean wind direction at 0.35 Hz to an onshore direction at 0.2 Hz.

As this case exhibited nearly ideal fetch-limited wave growth conditions in the presence of swell, it was selected for further investigation and comparison against established growth curves and model predictions in Chapters IV and V.

4. Case IV – 17 August 1997

Case IV, taken from the SandyDuck experiment, exhibits the most extreme effects of refraction and asymmetrical fetches. In this case, the mean wind speed varies spatially over the shelf from relatively light wind (~ 6-8 m/s) inshore at DUCN7 but increasing offshore (~ 8-12 m/s at 44014) and toward the south with the strongest winds near Cape Hatteras (~ 12-15 m/s at DSLN7) (Figure 7). As the mean wind direction is from the

southwest (~224^0) at a large oblique angle to the coastline (oriented 340/160), the fetch is asymmetrical about the wind direction. Waves generated from directions on the southern side of the mean wind direction will have considerably longer fetches than those generated with a more northerly component. As the winds and fetch are greatest to the south of the instrument locations, the dominant waves arriving at the 8M and 20M arrays (locations shown in Figure 3) are not locally forced, but generated by the stronger winds a few hundred kilometres to the south. These energetic waves, initially travelling offshore in the wind direction, undergo severe refraction over the shallow continental shelf bathymetry, resulting in a complete turning of the waves toward onshore propagation angles at the experiment site.

The strong refraction is evident in the frequency directional wave spectra observed at the 8M and 20M arrays (Figure 20). Waves at the 20M array are travelling almost alongshore, towards the north, approximately normal to the mean wind direction. The directional spread is very small as expected for the large refraction angle. By the time the waves reach the 8M array, they have been refracted further towards the shoreline and arrive at a slight southerly angle. The slanting ridge of energy apparent at the 8M array is further evidence of the significant refraction that is occurring at this location. At higher frequencies the 20M array shows evidence of a bimodal spectrum, caused by the two different sources of wave energy arriving at the array. One ridge of energy lies in the wind direction and is the result of the locally generated wind sea. The more energetic peak in the alongshore direction is caused by the arrival of waves generated off Cape Hatteras.

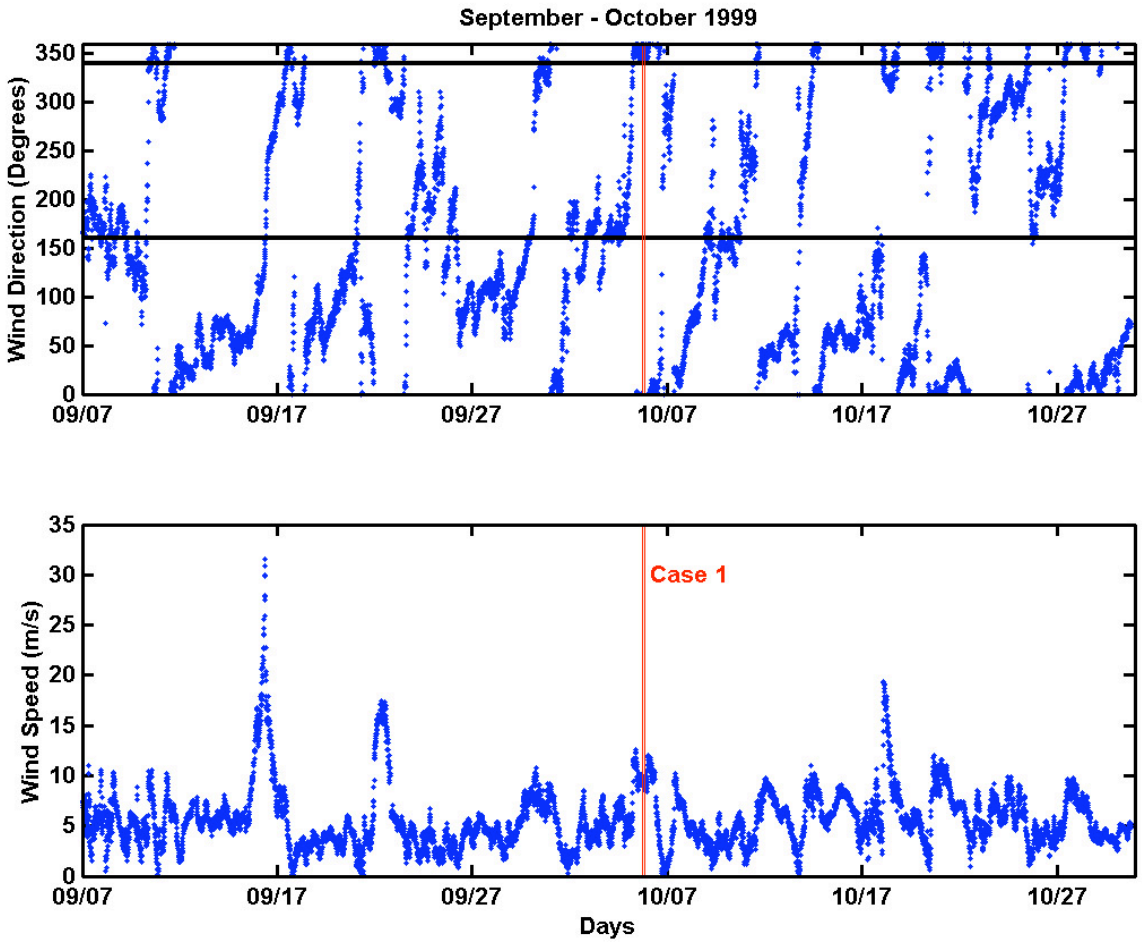

Figure 5. Wind speed and direction (from true north) observations from NDBC station DUCN7 during SHOWEX, September-October 1999. The black horizontal lines on the direction panel bracket the range for offshore winds and the red vertical lines indicate the cases selected.

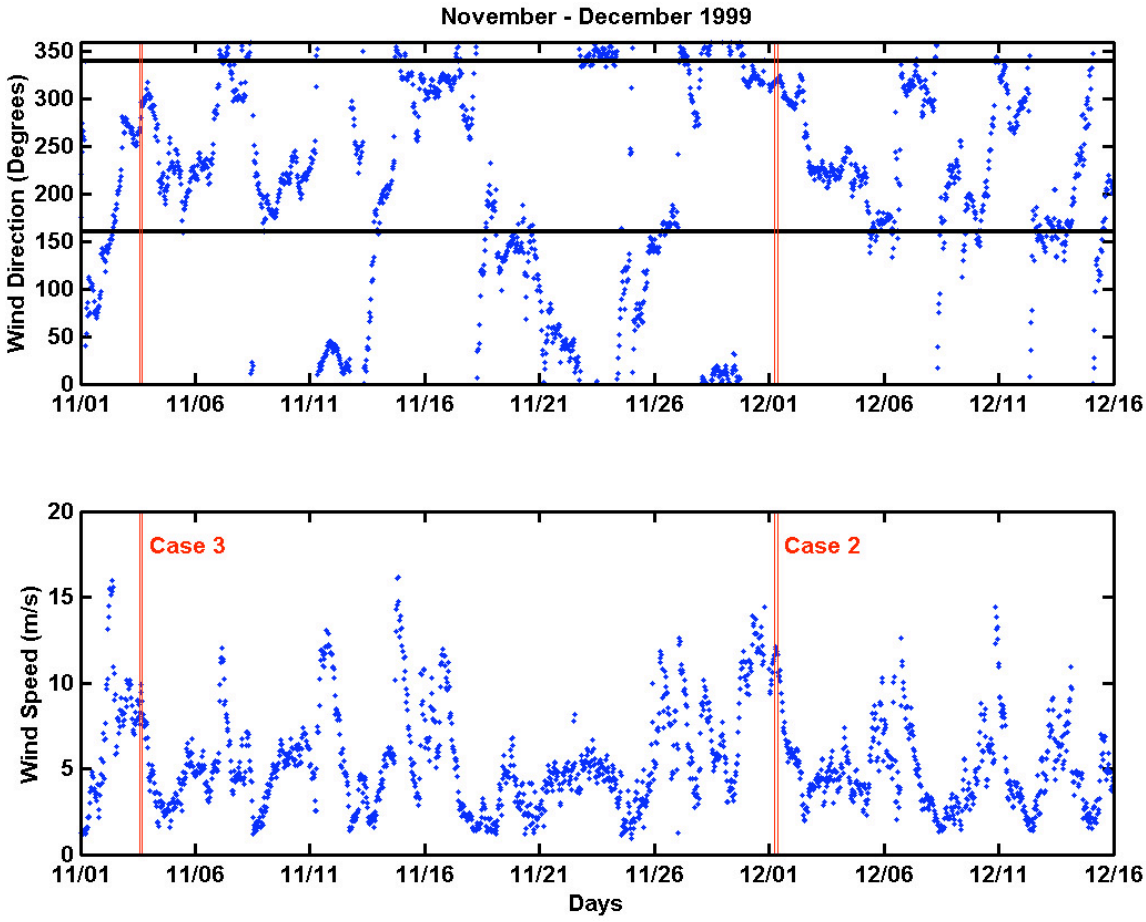

Figure 6. Wind speed and direction (from true north) observations from NDBC station DUCN7 during SHOWEX, November-December 1999. Same format at Figure 5.

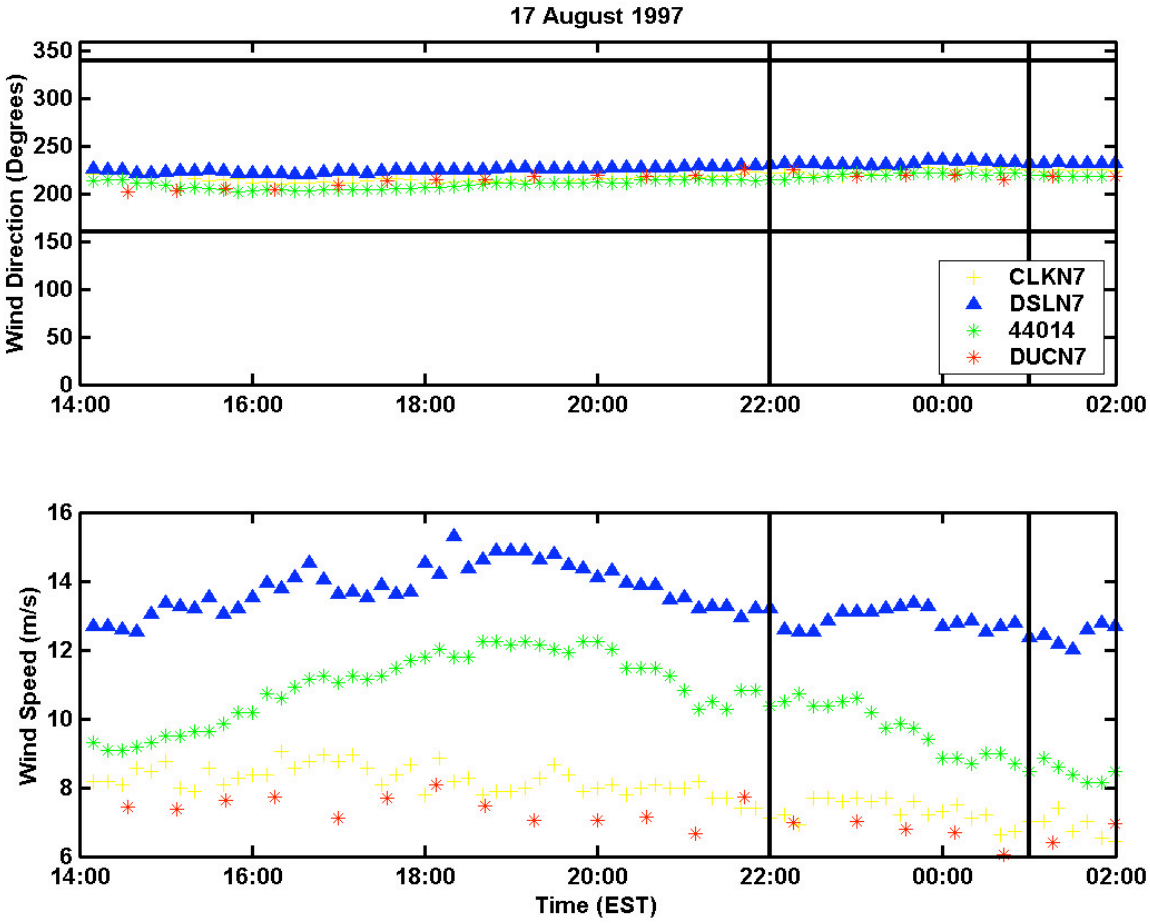

Figure 7. NDBC station wind speed and direction (from true north) observations over a twelve-hour period on 17 August 1997 (SandyDuck, Case IV). The black horizontal lines on the direction panel bracket the range for offshore winds and the black vertical lines indicate the selected time interval for Case IV.

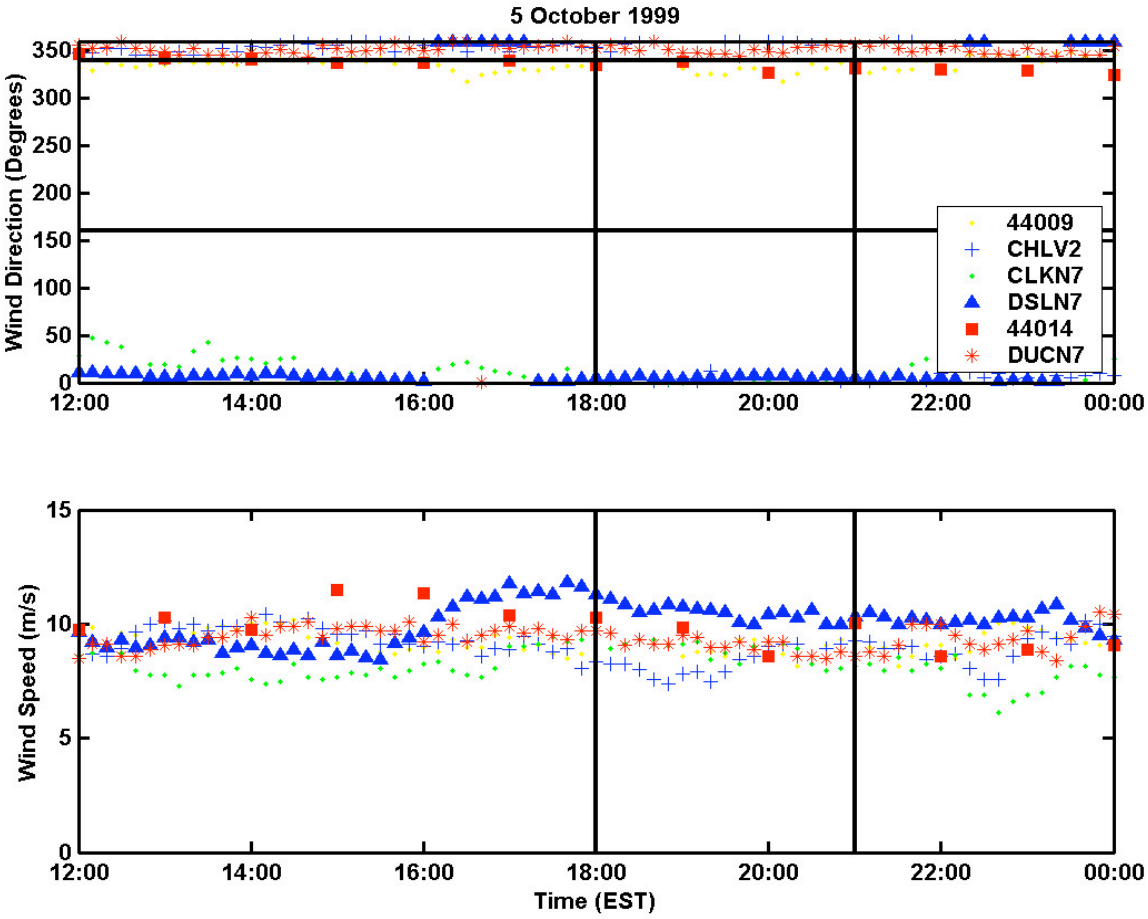

Figure 8. NDBC station wind speed and direction (from true north) observations over a twelve-hour period on 5 October 1999 (SHOWEX, Case I). Same format as Figure 7.

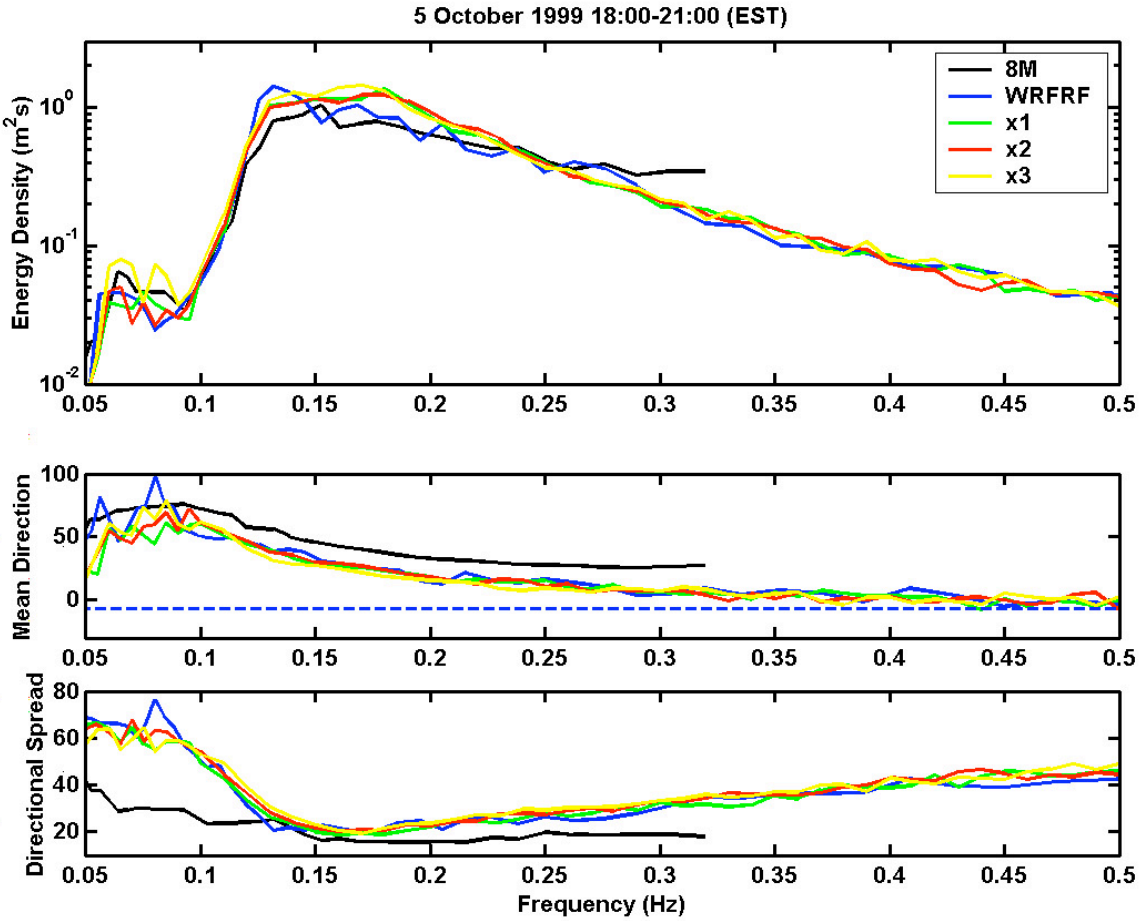

Figure 9. Energy density, mean wave direction (in degrees from true north) and directional spreading (in degrees) versus frequency for Case I. Estimates shown for the inner shelf instruments are based on a three-hour time period, indicated in Figure 8. The blue dashed line in the mean direction panel indicates the mean wind direction.

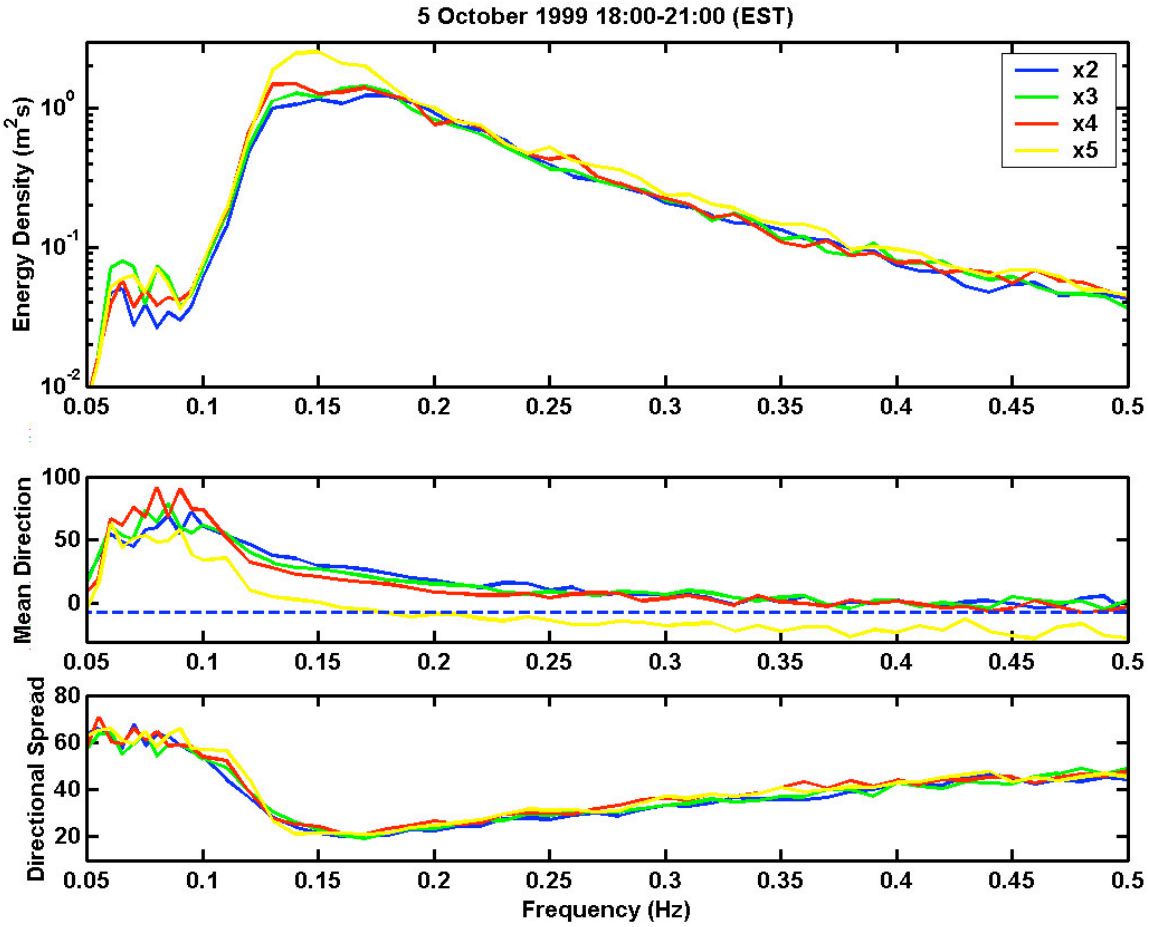

Figure 10. Energy density, mean wave direction (in degrees from true north) and directional spreading (in degrees) versus frequency for Case I. Estimates shown for the outer shelf instruments are based on a three-hour time period, indicated in Figure 8. Same format as Figure 9.

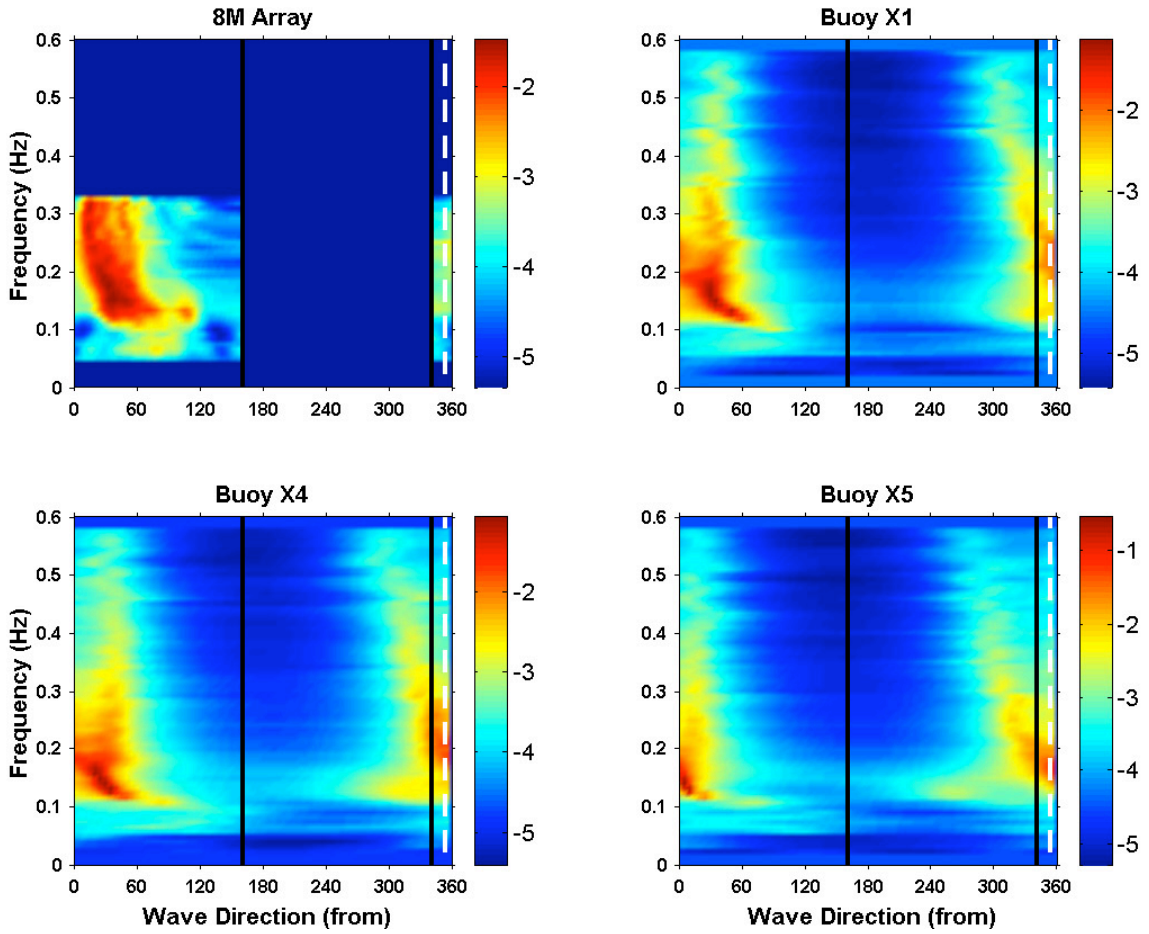

Figure 11. Frequency directional wave spectra observed at the 8M array and buoys X1, X4 and X5 in Case I. The black vertical lines bracket the range for offshore wind directions and the white dashed line indicates the mean wind direction. As the high frequency portion of the spectrum is attenuated at the sea floor, the array spectra were truncated at 0.32 Hz.

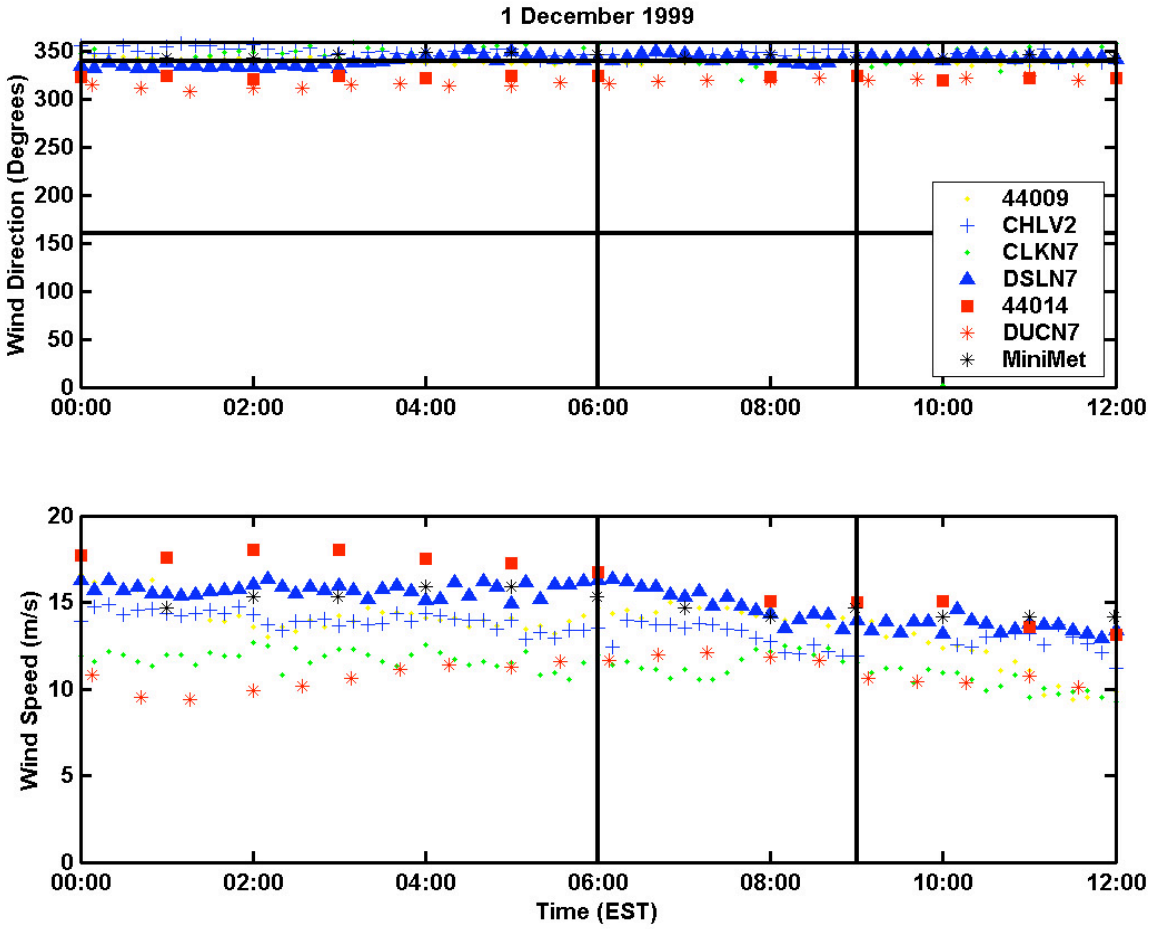

Figure 12. MiniMet buoy and NDBC station wind speed and direction (from true north) observations over a twelve-hour period on 1 December 1999 (SHOWEX, Case II). Same format as Figure 7.

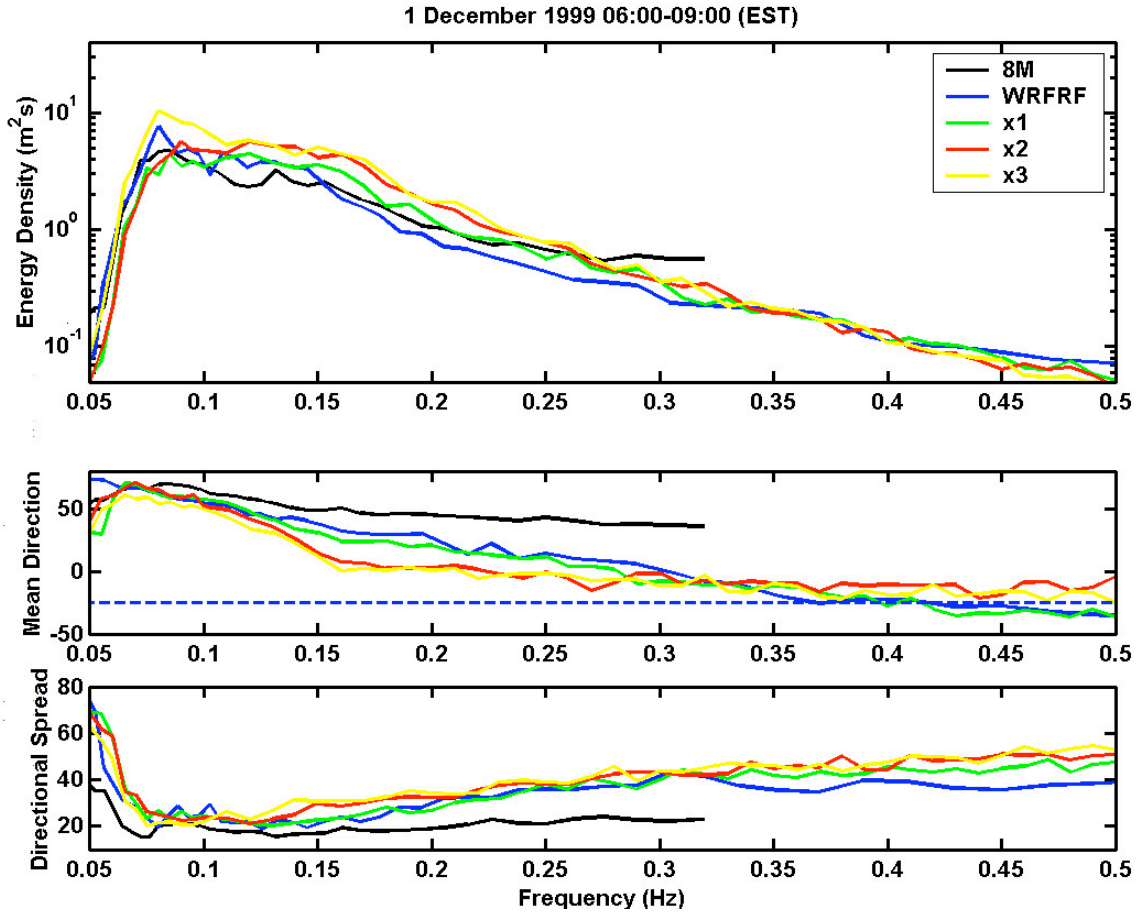

Figure 13. Energy density, mean wave direction (in degrees from true north) and directional spreading (in degrees) versus frequency for Case II. Estimates shown for the inner shelf instruments are based on a three-hour time period, indicated in Figure 12. Same format as Figure 9.

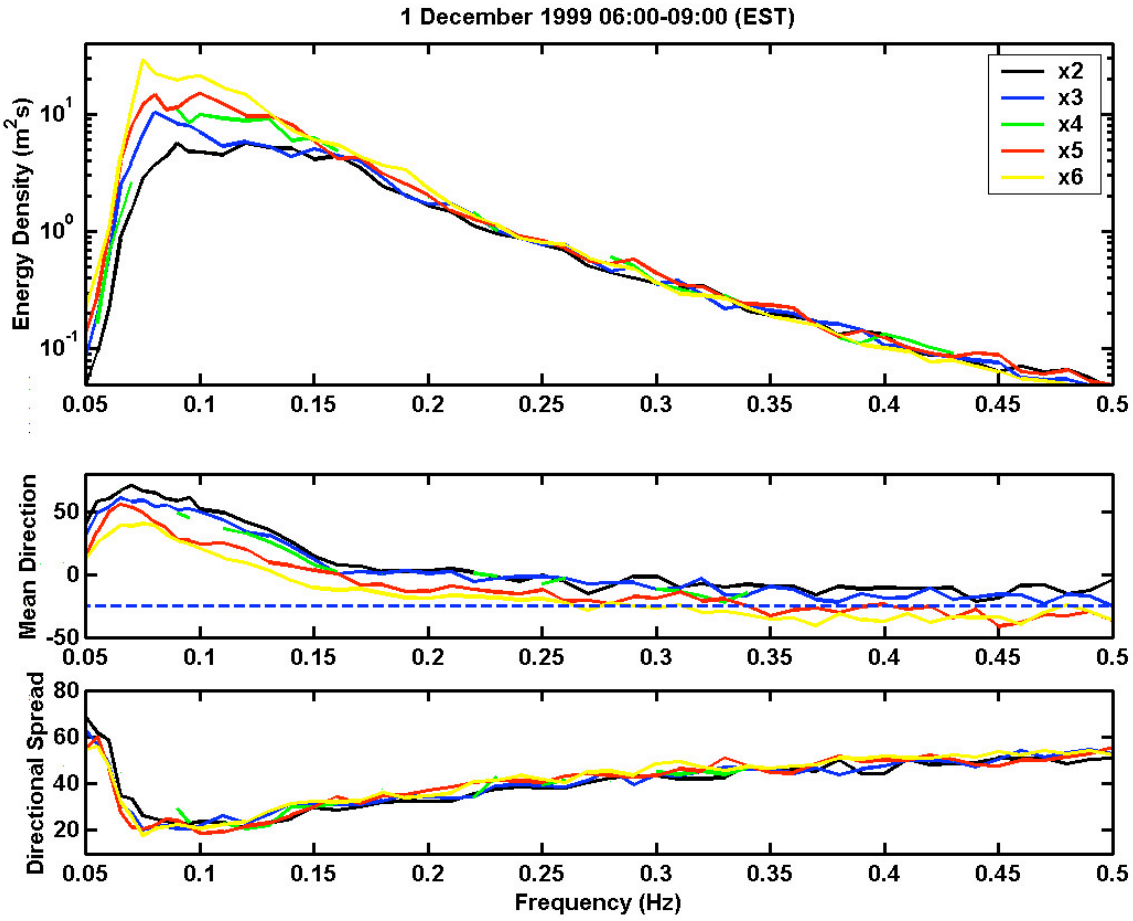

Figure 14. Energy density, mean wave direction (in degrees from true north) and directional spreading (in degrees) versus frequency for Case II. Estimates shown for the outer shelf instruments are based on a three-hour time period, indicated in Figure 12. Same format as Figure 9.

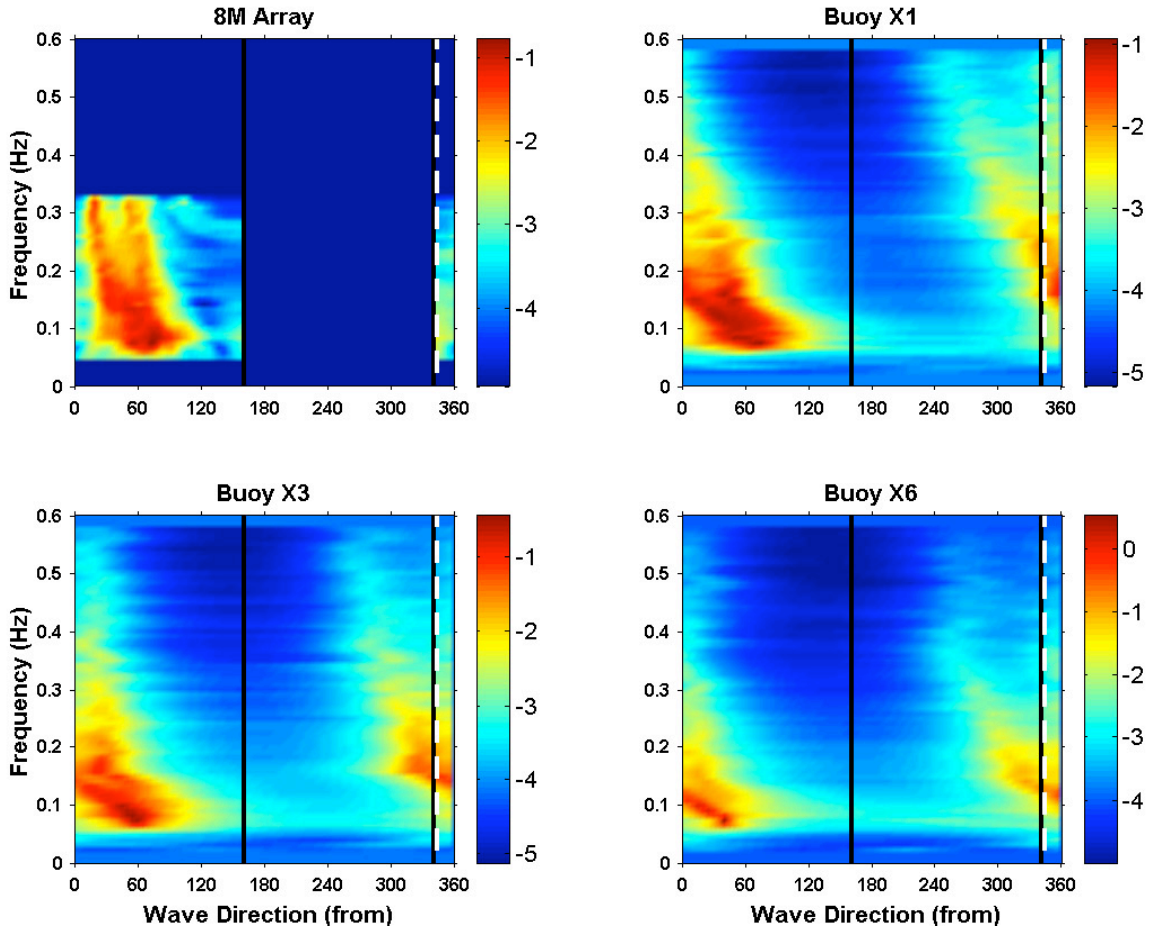

Figure 15. Frequency directional wave spectra observed at the 8M array and buoys X1, X3 and X6 in Case II. Same format as Figure 11.

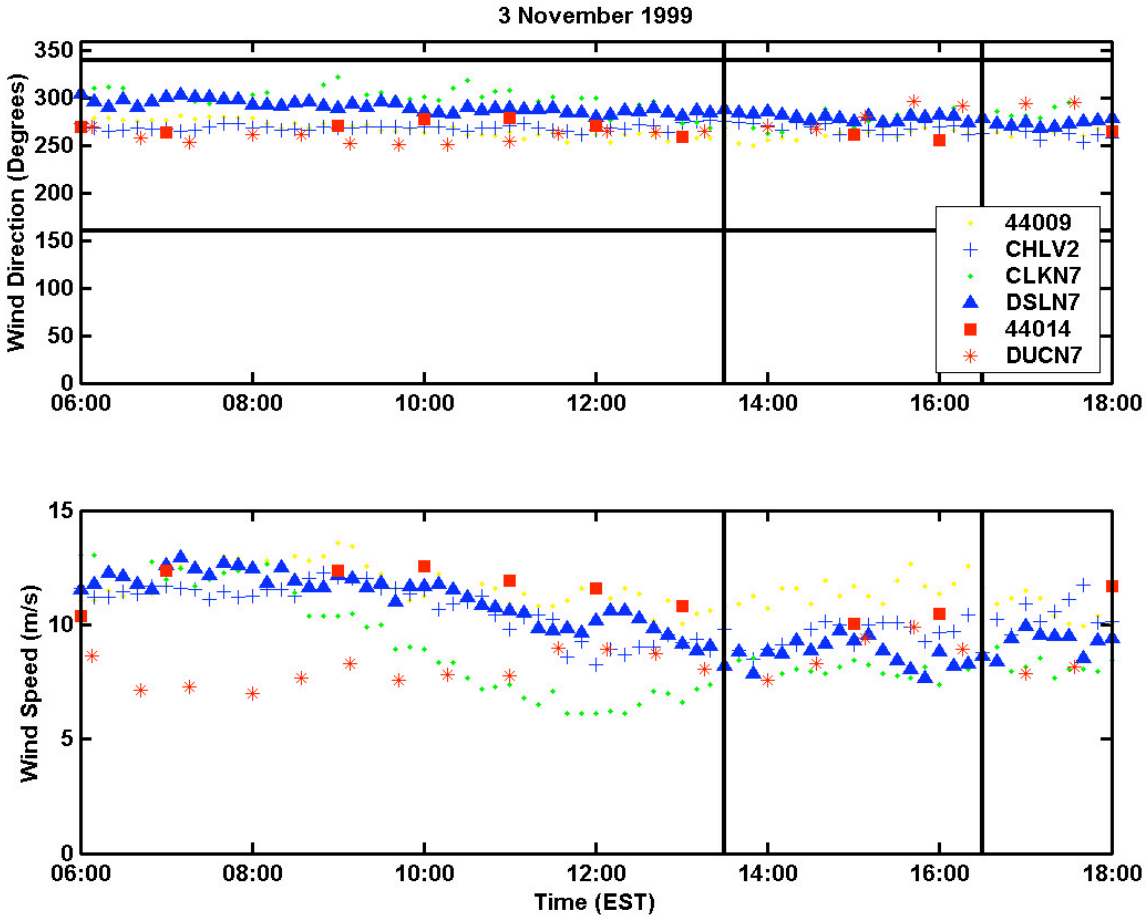

Figure 16. NDBC station wind speed and direction (from true north) observations over a twelve-hour period on 3 November 1999 (SHOWEX, Case III). Same format as Figure 7.

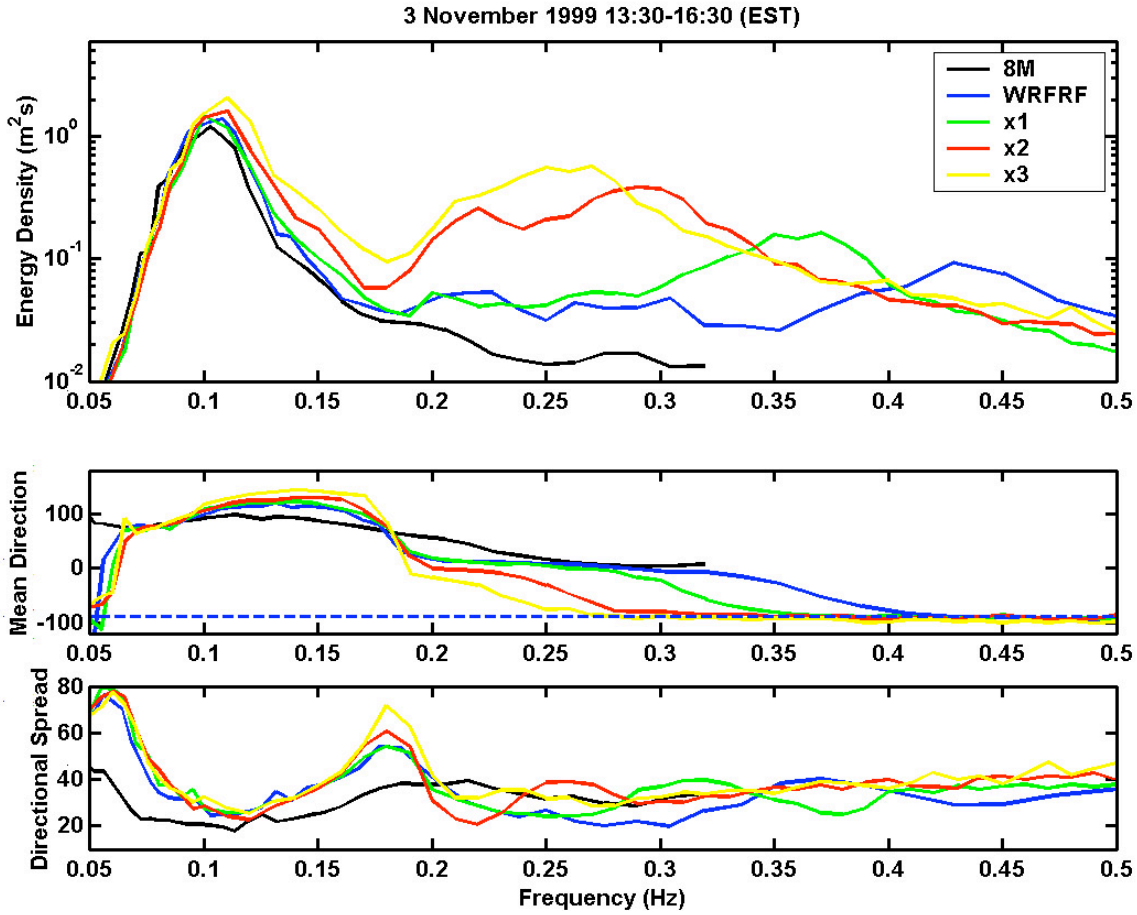

Figure 17. Energy density, mean wave direction (in degrees from true north) and directional spreading (in degrees) versus frequency for Case III. Estimates shown for the inner shelf instruments are based on a three-hour time period, indicated in Figure 16. Same format as Figure 9.

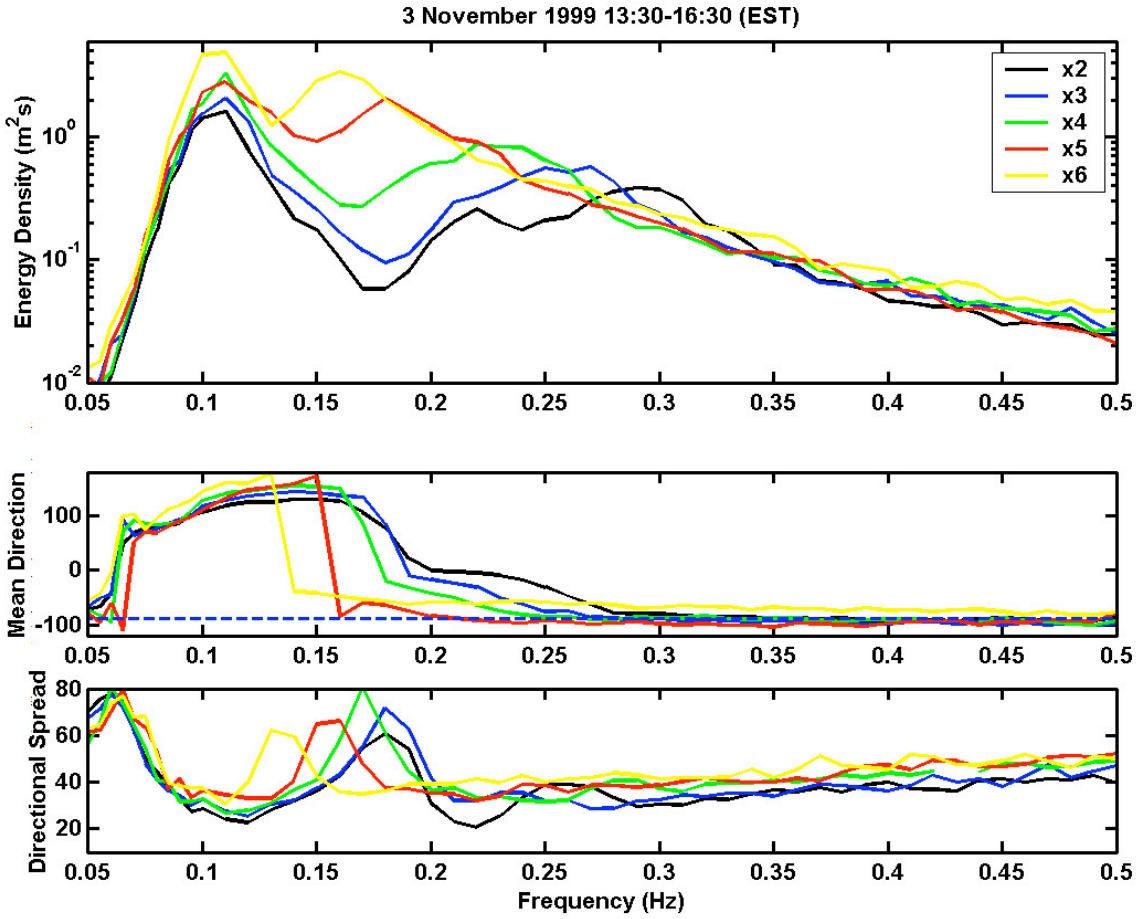

Figure 18. Energy density, mean wave direction (in degrees from true north) and directional spreading (in degrees) versus frequency for Case III. Estimates shown for the outer shelf instruments are based on a three-hour time period, indicated in Figure 16. Same format as Figure 9.

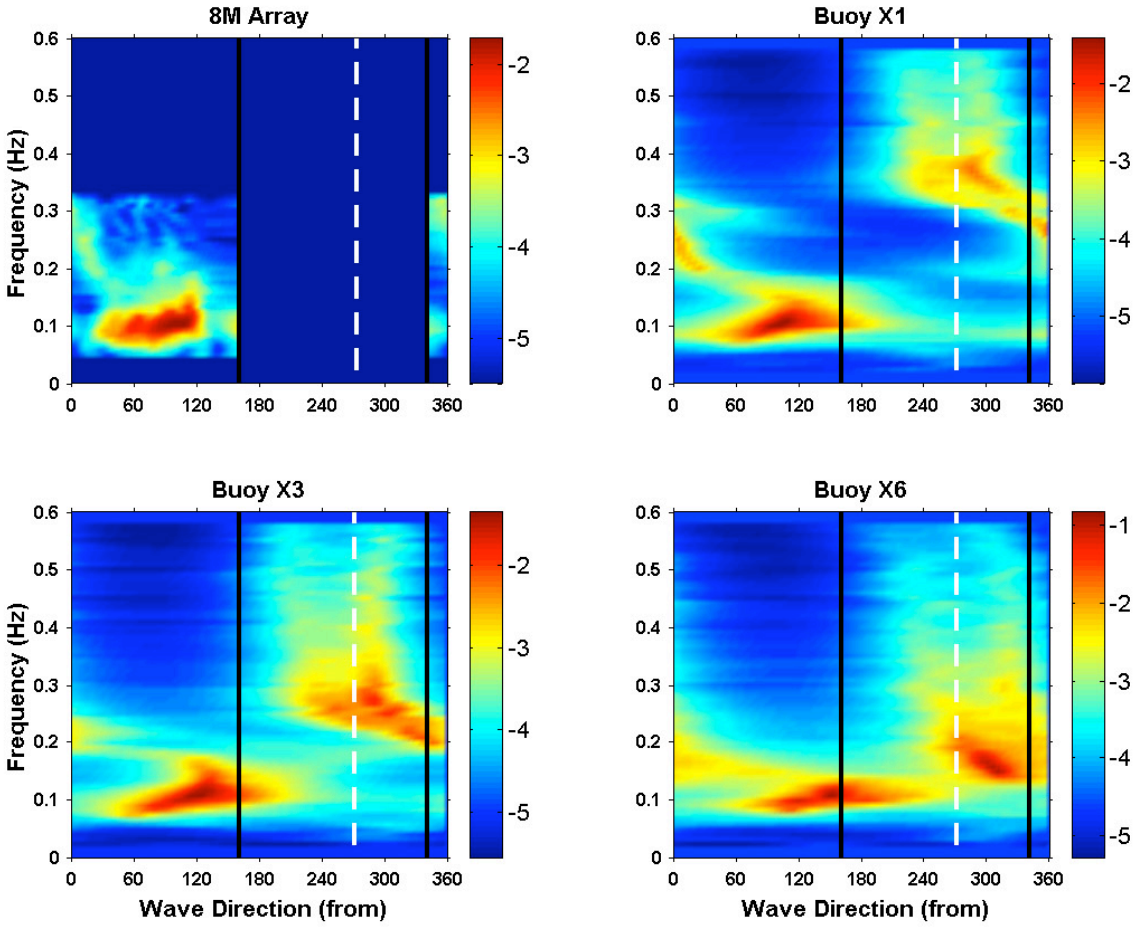

Figure 19. Frequency directional wave spectra observed at the 8M array and buoys X1, X3 and X6 in Case III. Same format as Figure 11.

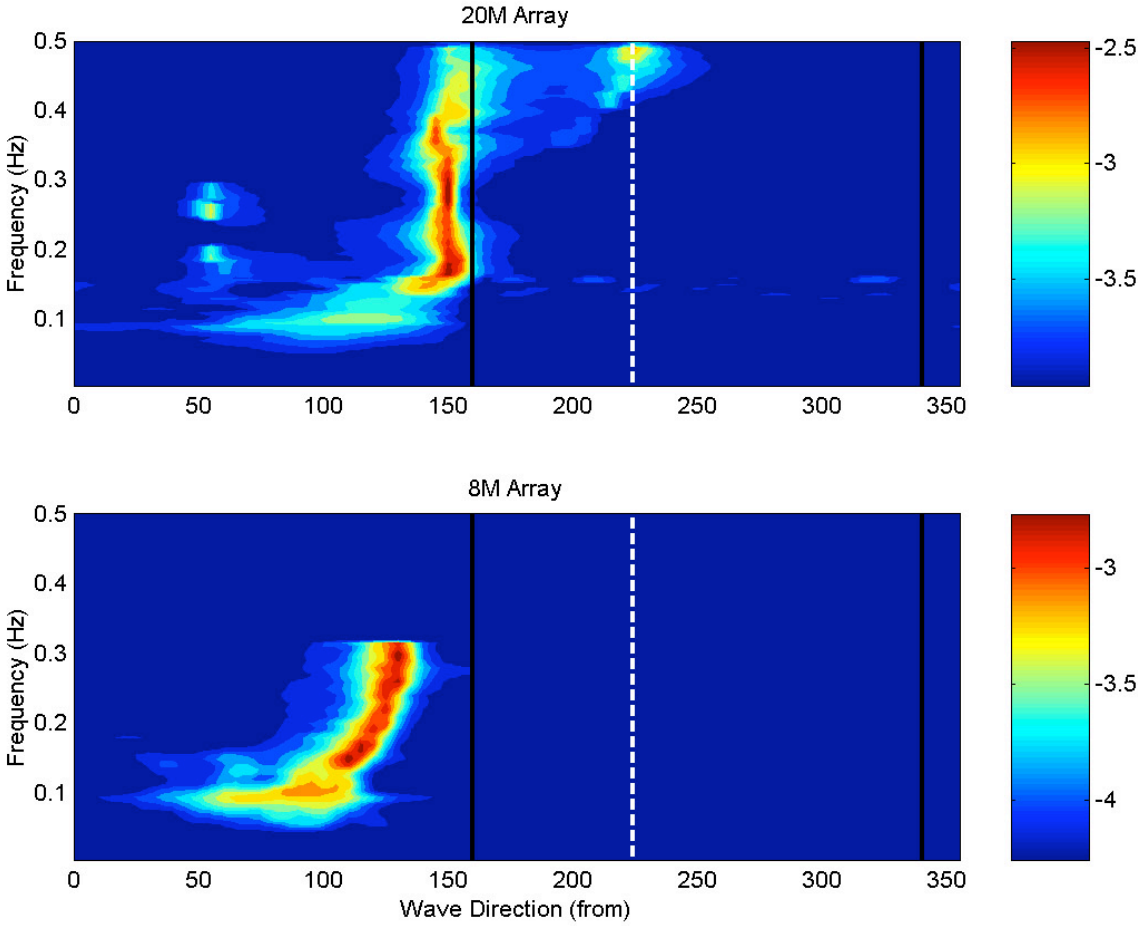

Figure 20. Frequency directional wave spectra observed at the 8M and 20M arrays in Case IV. The black vertical lines bracket the range for offshore wind directions and the white dashed line indicates the mean wind direction. As the high frequency portion of the spectrum is attenuated at the sea floor, the array spectra were truncated at 0.32 Hz (8M) and 0.16 Hz (20M). Data from the co-located directional Waverider at 20M were used to estimate the directional spectrum at frequencies higher than 0.16 Hz.

THIS PAGE INTENTIONALLY LEFT BLANK

IV. COMPARISON WITH GROWTH CURVES

As Case III (3 November 1999) featured nearly "ideal" offshore wind conditions similar to those detailed in the JONSWAP study, the growth rates and spectral characteristics are compared here with published fetch-limited growth relationships.

The earliest and most well-known relationships for fetch-limited wind wave growth are those proposed by Hasselmann et al. (1973). These consist of non-dimensionalised growth curves for energy, ($\tilde{E}$) and peak frequency, ($\tilde{f}$):

$$\tilde{E} = 1.6 \times 10^{-7} \tilde{X} \tag{9}$$

$$\tilde{f} = 3.5 \tilde{X}^{-0.33} \tag{10}$$

versus fetch, ($\tilde{X}$), which best fitted the JONSWAP observations. As the JONSWAP data was obtained during mostly stable atmospheric stratification, Kahma (1981) suggested that the growth relationship may vary, depending on whether the atmosphere is stable or unstable. In the Bothnian Sea experiment, conducted during unstable stratification, stronger growth was observed with best-fit curves:

$$\tilde{E} = 3.5 \times 10^{-7} \tilde{X} \tag{11}$$

$$\tilde{f} = 3.2 \tilde{X}^{-0.33}. \tag{12}$$

Kahma and Calkoen (1992) further examined the growth rates in numerous datasets and concluded that different growth curves existed for stable and unstable atmospheric stratification. They found that the relationship between energy growth and fetch is almost linear when the atmosphere is unstable, but the deviation from linear growth in a stable atmosphere is significant. They proposed the following growth rates for stable atmospheric stratification:

$$\tilde{E} = 9.3 \times 10^{-7} \tilde{X}^{0.76} \tag{13}$$

$$\tilde{f} = 1.9 \tilde{X}^{-0.24} \tag{14}$$

and for unstable stratification:

$$\tilde{\varepsilon} = 5.4 \times 10^{-7} \tilde{f}^{0.94} \tag{15}$$

$$\tilde{\varepsilon} = 2.3\tilde{f}^{0.28}. \tag{16}$$

In order to compare the observations for Case III with the above growth curves, the Bulk Richardson Number, in the form used by Kahma and Calkoen (1992) was calculated, as a measure of atmospheric stability:

$$R_b = \frac{g(T_a - T_w)/z_t}{T_a(U/z)^2} \tag{17}$$

Here T_a and T_w are the air and sea temperatures respectively, z is the height of the wind measurement and z_t is the height of the temperature measurement. The air and sea temperatures were obtained from the standard meteorological data historical archive files for NDBC station 44014 (NDBC, 2003) and these values, as well as the calculated Bulk Richardson number, are shown in Figure 21. Over the entire twelve-hour period, the sea temperature was consistently O[10^0 C] warmer than the air temperature, resulting in a statically unstable atmosphere.

To construct growth curves of energy density and peak frequency versus fetch, the fetch for each instrument location needed to be determined. The average wind speed and direction for this case was calculated over the three-hour case time (1330-1630) using wind observations from the four wind stations closest to the SHOWEX transect at DUCN7, CHLV2, DSLN7 and 44014. As the coast is a long, straight chain of barrier islands, in order to determine the fetch, the baseline coast was approximated with a straight line along the seaward side of the North Carolina Outer Banks, oriented 340/160 from true north. The fetch was estimated to be the distance along the wind direction (~270^0), between each instrument location and the intersection point on the coastline. The fetch for each location is shown in Table 5.

Instrument	Fetch (km)
WRFRF	3.93
X1	6.04
X2	14.20
X3	23.55
X4	37.20
X5	56.21
X6	82.05

Table 5. The calculated fetch for Case III.

As the observations used in this study also include a component of swell energy, the spectra needed to be partitioned into separate sea and swell components. For each instrument a trough between the sea and swell peaks was located, and the energy to the left of this point was removed. In the case of X2 to X6, the separation between the two peaks was quite distinct, and the spectra were easily separated. For buoy X1 and WRFRF however, the region between the swell and the wind wave peak was rather broad, and it was difficult to determine a distinct separation point. For these two cases the partitioning was done somewhat arbitrarily. The wind sea spectra for these two locations may therefore contain a small amount of residual swell energy. Figure 22 shows the energy density spectrum across the entire range of frequencies, as well as the remaining "wind sea" spectrum that was left after removal of the swell energy. This part of the spectrum was then used in the growth curve calculations.

The fetch, energy and peak frequency were non-dimensionalised using Equations 3-5 (with a mean wind speed of $U = 9.3\ m/s$). The results are compared in Figure 23 with the JONSWAP, Kahma (1981) and (unstable) Kahma & Calkoen (1992) relationships. The data appears to best fit the relationships developed by Kahma (1981) from the Bothnian Sea experiment where atmospheric stratification was also unstable.

The good agreement with established growth curves is surprising considering the presence of energetic swell with a propagation direction that opposes the wind wave direction. These results indicate that the presence of swell may not have a strong effect on

fetch-limited wind wave growth, contradicting results in earlier laboratory experiments (Holthuijsen, 2000; and references therein).

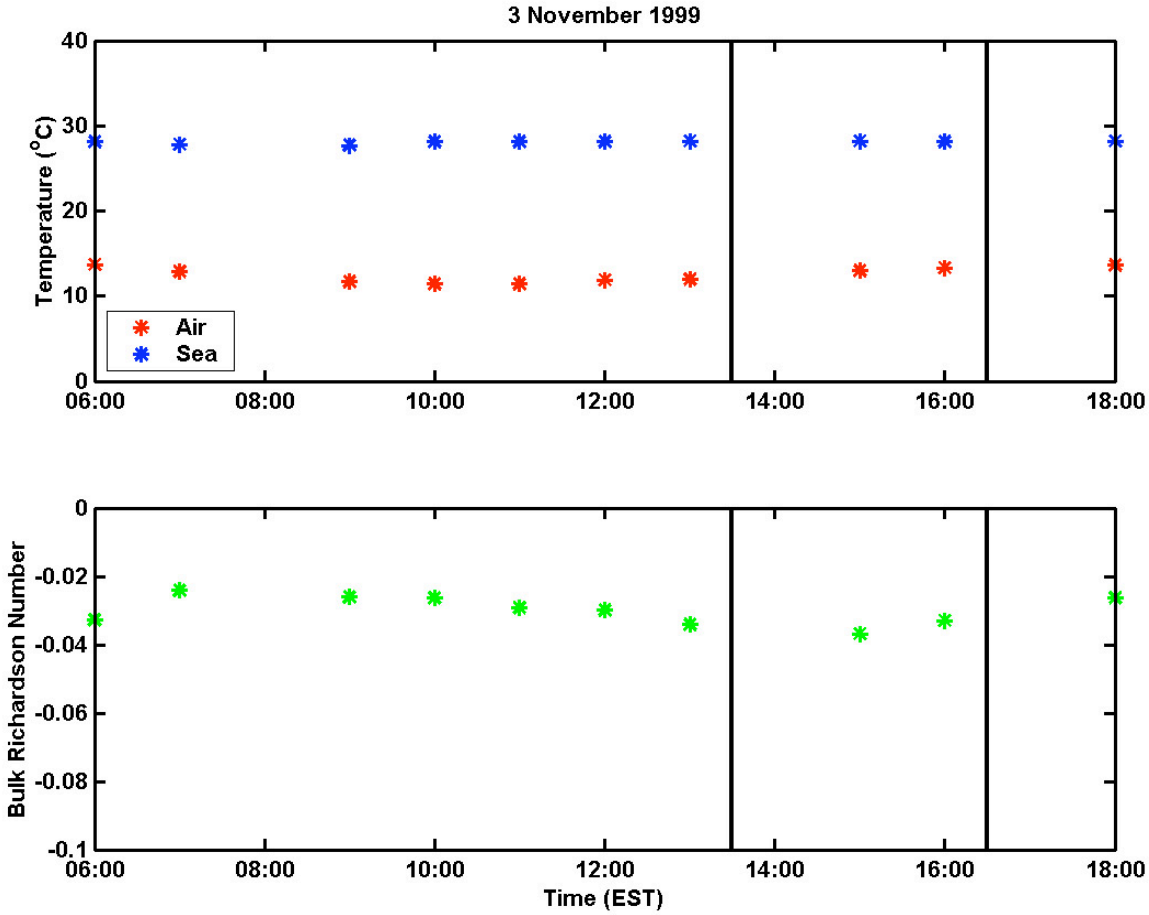

Figure 21. Air and sea temperature, and estimated Bulk Richardson Number at NDBC station 44014 for a twelve-hour time period on 3 November 1999. The black vertical lines indicate the three-hour time period for Case III.

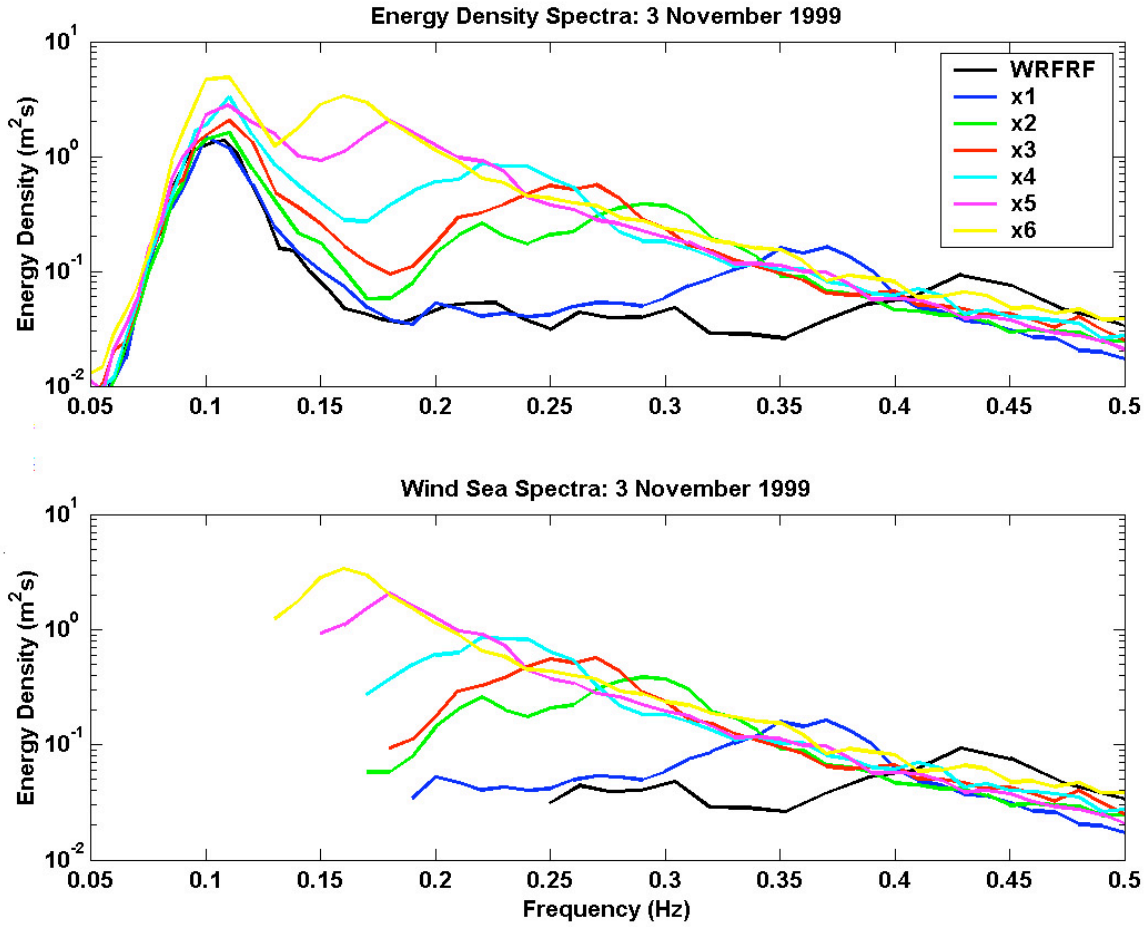

Figure 22. Energy density spectra for Case III (Panel a.) and the truncated wind sea spectra (Panel b.), after the swell component has been removed.

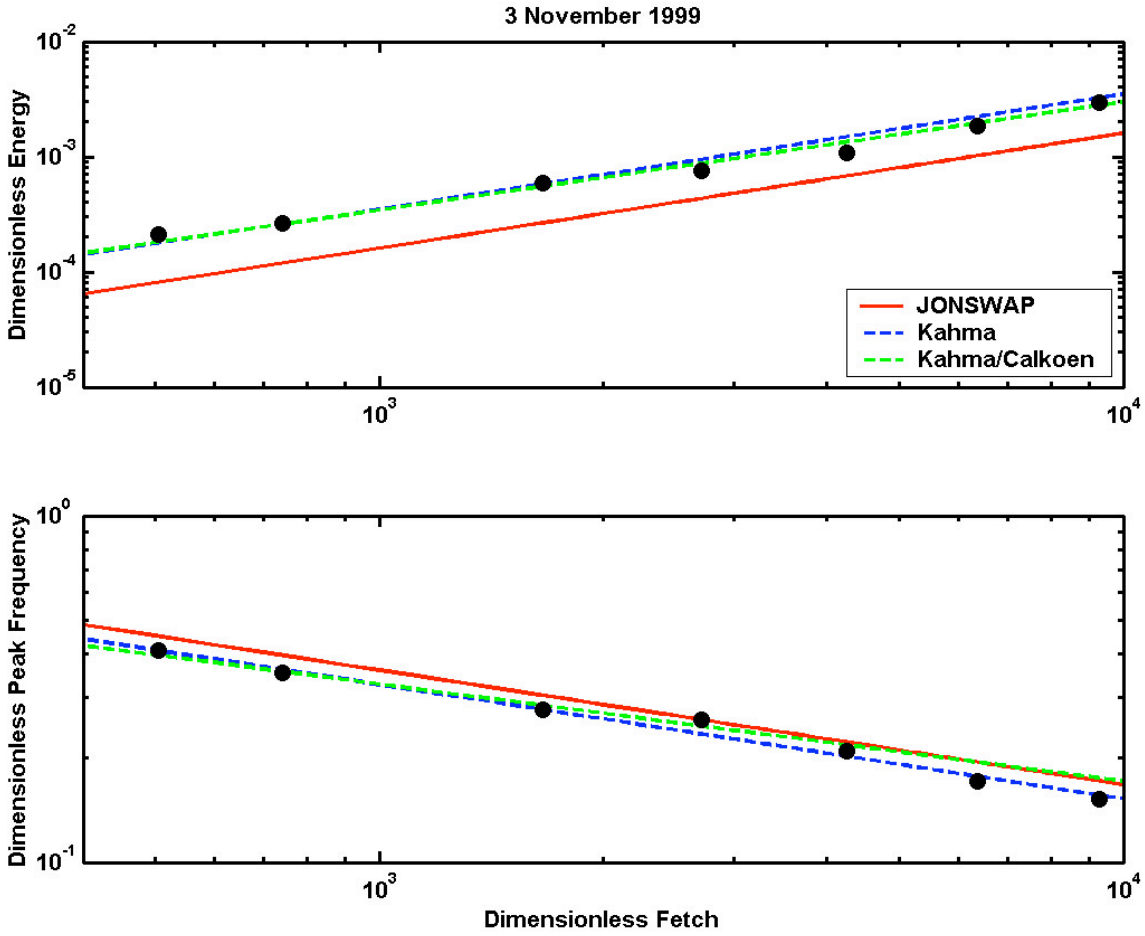

Figure 23. Dimensionless energy and peak frequency versus dimensionless fetch for SHOWEX observations over the three-hour time period of Case III. Previously formulated growth relationships from the literature are also shown for comparison.

THIS PAGE INTENTIONALLY LEFT BLANK

V. COMPARISON WITH MODEL PREDICTIONS

Third generation numerical wave models are the state of the art tools for predicting wind wave evolution across ocean basins and on smaller regional scales. This type of model is a vast improvement over first generation models, which did not account for nonlinear energy transfers across the spectrum, and second generation models, which included a simple parameterisation for nonlinear transfers and placed limitations on the shape of the wind sea spectrum (Tolman, 1991). Third generation models provide a full discrete spectral resolution model for the propagation, generation and dissipation of two-dimensional wind wave spectra by integrating the basic energy transport equation:

$$\frac{\partial F}{\partial t} + \nabla_{\vec{x}} (c_{\vec{x}} F) + \nabla_{\vec{k}} (c_{\vec{k}} F) = S \tag{18}$$

from first principles, using defined source functions and without placing any restrictions on the spectral shape. The energy density, $F(t,\vec{x},\vec{k})$, is a function of time, t, the horizontal position vector, $\vec{x}$, and the wavenumber vector $\vec{k}$. The first term in this equation describes the local rate of change and the second and third terms describe propagation effects in terms of the divergence of energy fluxes in the physical, $\vec{x}(x,y)$, and spectral, $\vec{k}(f,\theta)$, space respectively, where $c_{\vec{x}}$ and $c_{\vec{k}}$ are the corresponding energy transport velocities. The right hand side of Equation 18 represents the sum of the source terms:

$$S = S_{in} + S_{nl} + S_{ds} \tag{19}$$

which generally includes the effects of wind input, S_{in}, nonlinear wave-wave interactions, S_{nl}, and dissipation, S_{ds}. Additional source terms such as wave-bottom interactions and bottom friction, S_{bot}, can also be added for shallow water applications (see Komen et al. (1994) for a detailed account of the theory).

The WAM model (WAMDI Group, 1988) was the first operational third generation model and was calibrated against fetch-limited wave growth data from the JONSWAP experiment. Subsequently developed third-generation models contain much

of the same physics and parameterisations with refinements in numerical techniques and alternative wind input and dissipation source terms. Here we use the WAVEWATCH III model.

A. WAVEWATCH III

WAVEWATCH III is an operational third generation ocean wave model that was developed by H. L. Tolman and colleagues at the U.S. National Oceanic and Atmospheric Administration's (NOAA) National Centers for Environmental Prediction (NCEP). It is a further development of the earlier versions WAVEWATCH I, developed at Delft University of Technology, and WAVEWATCH II, developed at NASA Goddard Space Flight Centre, and includes numerous refinements in the structure of the model, its governing equations, numerical methods and physical parameterisations (Tolman, 2003). WAVEWATCH III Version 2.22 was used for model-data comparisons in this study and a brief outline of the model's source terms is presented in the following discussion. A complete reference for the model physics, governing equations, numerical schemes and source terms can be found in the user manual and system documentation of WAVEWATCH III version 2.22 (Tolman, 2002).

B. SOURCE TERMS

Whilst the nonlinear interaction and wind input source terms in Equation 19 are based on sound physical theories and have been studied extensively, the dissipation term, which accounts for the loss of energy due to wave breaking, is poorly understood and represented with simple empirical parameterisations. WAVEWATCH III also includes an additional fourth term, S_{bot}, which accounts for bottom friction in shallow water (Tolman, 2002). Modifications and empirical fine-tuning of the source terms has led to several alternative formulations. In the present study we use the well-established source terms of the WAM model as well as the more recent formulation proposed by Tolman and Chalikov (1996). Differences between these formulations are summarised below.

1. Nonlinear Interactions (S_{nl})

To accurately calculate the nonlinear interaction source term in any wind wave model, a six-dimensional Boltzmann integral must be computed. Since this evaluation is computationally prohibitively expensive for use in operational models, Hasselmann et al.

(1985) developed the Discrete Interaction Approximation (DIA), which parameterises this term in terms of a few interactions. The DIA, first used in the WAM model, was adopted in the WAVEWATCH III and many other models.

2. Wind Input (S_{in}) and Dissipation (S_{ds})

The energy balance between the wind input and dissipation source term is considered to be important for modelling wave growth as the two source terms are interconnected, although they represent two distinct processes. Wind input and dissipation are therefore treated as a collective source term in the WAVEWATCH III model (Tolman, 2002). Two different forms of the combined source terms are available when running the model. The WAM-3 combination of source terms, used in cycles 1 to 3 of the WAM model contains a wind input formulation based on experiments by Snyder et al. (1981) and a simple semi-empirical dissipation term proposed by Komen et al. (1984). The JONSWAP growth curves were used to tune the dissipation source term so that it reproduced previously observed fetch-limited wind wave observations (WAMDI Group, 1988).

Tolman and Chalikov (1996) presented an alternative parameterisation based on the argument that the dissipation processes for frequencies at and below the spectral peak are inherently different from those occurring at higher frequencies. Their dissipation source term contains two distinct components, for these two frequency regimes. At the low-frequency end of the spectrum, dissipation assumes a form similar to the dissipation of wave energy caused by turbulence in the oceanic boundary layer. For the high-frequency region, a diagnostic parameterisation is applied, which is modelled on the power-law behaviour of the observed spectral tail. The resulting source term is a linear combination of these two components, and for continuity, a transition zone is defined between the high- and low-frequency components (see Tolman and Chalikov, 1996, for further details).

3. Bottom Friction (S_{bot})

The source term describing dissipation due to bottom friction is parameterised according to an empirical relationship derived from the JONSWAP study (Hasselmann et al., 1973). This formulation is used in WAVEWATCH III and WAM (Tolman, 2002).

C. MODEL SET-UP

During the SHOWEX experiment, COAMPS wind fields with 0.2^0 resolution were obtained from the U.S. Navy's Fleet Numerical Meteorology and Oceanography Centre (FNMOC) and these data were used as the wind forcing in the WAVEWATCH III model for this study. A six-hour time step was used for the wind information, and therefore, the 00 and 12 UTC data values were taken from the COAMPS analysis cycle, whilst the 06 and 18 UTC values were obtained from the forecast cycle. As the 00 and 06 UTC data on 4 November 1999 were missing, the forecast from the 12 UTC cycle was used instead to interpolate the winds at these two times.

Figure 24 compares the NDBC observations of wind speed and direction, with the COAMPS predictions at the nearest grid points for Case III. The COAMPS data show relatively good agreement with the actual wind direction observations, but the wind speeds are a little more variable. The model field at 1300 EST is shown in Figure 25(a). Even though there are some discrepancies, the COAMPS winds do capture the weaker inshore and stronger offshore winds as observed by the NDBC stations. In addition to model runs forced with COAMPS winds, model runs forced with homogeneous winds, using the average observed wind speed and direction over the three-hour case time (9.3 m/s and 270^0), were performed to examine the importance of spatial variability in wind conditions.

The bathymetry data used in the model grid was obtained from a variety of sources including the National Geophysical Data Centre (NGDC) high-resolution digital bathymetry data archive and a number of dedicated surveys that were conducted during the DUCK94 Nearshore Processes Experiment and SHOWEX (see Herbers et al. (2000) and Ardhuin et al. (2003) for details).

The WAVEWATCH III model domain used in this study covers the area of the North Carolina/Virginia continental shelf shown in Figure 25(b), with a two-minute grid resolution. The wave spectra were discretised into 24 directions and 30 frequencies. The directions start at true north and encompass 360^0 clockwise in increments of 15^0. The lowest frequency is 0.041 Hz and they are logarithmically incremented by a factor of 1.1. A two-minute time step was used for integrating both the propagation and source terms.

In order to account for the arrival of swell from the open ocean, the model was forced at the offshore boundary with data from buoy X6. Swell frequency-directional spectra were estimated from one-hour buoy records using the Maximum Entropy Method (Lygre and Krogstad, 1986). These data were applied without any time lag along the offshore boundary.

D. MODEL/DATA COMPARISON

Model-data comparisons are presented here for Case III, which exhibited classic fetch-limited wave growth conditions. A number of model runs were carried out in order examine the effects on wind wave growth of different source terms and also the presence of swell. A total of twelve runs with combinations of the following model settings were conducted:

- Wind – COAMPS versus homogeneous winds or no wind;
- Atmospheric Stability – stable versus unstable;
- Source Term – WAM-3 versus Tolman and Chalikov (T&C);
- Bathymetry – flat bottom versus actual bathymetry; and
- Swell – pure wind sea versus inclusion of actual swell.

Seven of these runs listed in Table 6 are discussed in detail in the following section.

Run	Description	Wind	Stability	Source Term	Swell
1	WAM/Homog	270/9.3 m/s	Stable	WAM-3	No
2	WAM/COAMPS	COAMPS	Stable	WAM-3	No
3	T&C/COAMPS	COAMPS	Stable	T&C	No
4	T&C/COAMPS/Unstable	COAMPS	Unstable	T&C	No
5	WAM/COAMPS/SWELL	COAMPS	Stable	WAM-3	Yes
6	T&C/COAMPS/Unstable/SWELL	COAMPS	Unstable	T&C	Yes
7	WAM/NO WIND/SWELL	None	Stable	WAM-3	Yes

Table 6. Description of model runs.

All of the above listed runs were conducted using the actual bathymetry over the continental shelf. Some additional runs, not shown here, were carried out using a 100 metre flat shelf but differences in the predicted wind wave growth between the runs with and without bathymetry were small, with the exception of the nearshore region that is not well resolved by the model. In the unstable atmosphere runs, a correction factor ($\prod 10^{0}C$) was applied to reflect the actual difference between the measured air and sea temperatures.

In order to separate the swell and sea contributions of the predicted spectra, the same cut-off frequency used for separating the wind sea and swell components in the actual data (discussed in Chapter IV), was applied to the model results The following model/data comparison discussion is broken into two parts. The first section compares observations with model results for only the wind sea part of the spectrum, while the second part discusses the effect of swell on predicted wind wave growth.

1. Comparison of Model Predictions with Observations and Empirical Growth Curves

In order to compare the results of the model runs with previously published fetch-limited growth relationships, only the wind sea component of the spectrum was considered. Figures 26 and 27 show dimensionless energy and peak frequency respectively as a function of nondimensional fetch, for the observed data, growth curves in the literature and model Runs 1-4. Results using COAMPS winds (Run 2) are generally in better agreement with observations than predictions based on a homogeneous wind (Run 1). The homogeneous wind (Run 1) better fits the observations, only at the two shortest fetches (WRFRF and X1), whilst Run 2 which uses the COAMPS winds, overestimates the energy growth and underestimates the peak frequency. There are two possible causes for this discrepancy near the coast. First, the barrier islands are not well resolved by the COAMPS wind model and the coastal lee effect may not be well represented. Thus wind predictions near the shore may be biased high, resulting in an overestimate of the wave growth at short fetches. Spurious growth at the shortest fetches may also result from the poor wave model resolution at the coast. Buoys WRFRF and X1 are only a few grid points from the coast, and hence, the model may not resolve the

wave growth and the refraction over these short fetches. Higher resolution models are needed to accurately represent the nearshore wave evolution.

Runs 1 and 2 use the WAM-3 source term, which is known to flatten the growth curve compared to the empirical JONSWAP relationship, causing an overestimation of energy at short fetches and underestimation of energy at longer fetches. As the peak frequency evolves as the result of non-linear transfers to lower frequencies, an increase in energy will cause a decrease in peak frequency, and hence the peak frequency will be underestimated. These trends are consistent with the hindcast results shown in Figures 26 and 27.

In Run 3, using the alternative T&C source term, the energy is underestimated across the entire spectrum. Compared with the WAM-3 source term, the errors at longer fetches are reduced and do not increase with fetch. At longer fetches, the slope is comparable to that of the Kahma and JONSWAP relations and does not tend to flatten out as observed with the WAM-3 source term. When the T&C source term is forced with COAMPS winds, including a correction for atmospheric instability (Run 4), the results for the growth of energy are close to the observed values. This run appears to exhibit the most accurate representation of the observations across the entire shelf. For the peak frequency, the shortest fetches are better modelled by the T&C source term (Run 4), but at longer fetches results for the two source terms (forced with COAMPS winds) are similar (Runs 2 and 4).

2. The Effect of Swell

The winds offshore in Case III oppose the energetic swell arriving from the Atlantic Ocean. Hence additional model runs were conducted that include swell, in order to investigate its effect on the predicted growth of the wind wave spectrum. Figures 28 and 29 compare predictions of wind sea energy and peak frequency in the presence of swell using the WAM-3 (Run 5) and T&C (Run 6, with unstable atmosphere) source terms respectively. Also included is Run 2, discussed earlier, which uses the same WAM-3 source term as Run 5 but without swell, as a benchmark for wave growth in the absence of swell.

By comparing Runs 2 and 5 (WAM-3), it is noticeable that with the inclusion of swell (Run 5) the energy is significantly overestimated across the entire wind sea spectrum and the peak frequency is underestimated. To quantify the contribution of swell in the combined wind sea and swell model results, an additional Run 7 was conducted without wind. The predicted swell energy levels in the wind sea band are relatively small (compared with Runs 5 and 7 in Figure 28), indicating that the inclusion of the swell energy causes the wind sea to grow unrealistically. This effect has been observed before (Holthuijsen et al., 2000) and can be explained by the way in which the WAM-3 source term models the dissipation due to whitecapping. Here, whitecapping depends on the mean steepness of the waves. With the addition of the low frequency swell into the spectrum, the mean wave steepness is reduced and hence less dissipation is predicted. The resulting unbalanced wind input and dissipation causes increased wind sea growth that is not observed.

For Run 6, the Tolman and Chalikov source term was used in conjunction with the COAMPS wind fields (including an instability correction) and the presence of a swell. This run most accurately represents the physical situation and yields the best overall agreement with the observations with the exception of a bias in the peak frequency, which is underestimated at the shortest fetches and overestimated with increasing fetch. Whilst the WAM-3 source term shows a significant difference between the model results with and without the presence of swell, the T&C runs with (Run 6) and without (Run 4) swell, yield similar results indicating that the addition of swell has a small effect on the wind wave growth, which is supported by the observations.

Predictions of energy density, mean wave direction and directional spread, as a function of frequency, at buoy X2 using Wam-3 (Run 5) and T&C (Run 6) source terms, are compared with observations in Figure 30. Buoy X2 was selected for this comparison because it is close to the coast so wave growth will be influenced by refraction, but results are unlikely to be affected by poor model grid resolution. Whilst both model runs accurately reflect the position of the swell peak, although slightly underestimating the energy level, the wind sea region of the spectrum is not well modelled. The observed spectrum exhibits two distinct energy peaks representing the swell and wind sea with a smaller peak in between, possibly caused by refraction of wind waves close to the coast.

Run 6 (T&C) underestimates the energy levels at the intermediate frequencies between the dominant swell and sea peaks, showing a deep trough in the spectrum that is not observed. In comparison, Run 5 (WAM-3), tends to overestimate the energy across the wind sea frequencies but does not exhibit such a large discrepancy at the energy minimum.

The mean wave direction observations at buoy X2 show the effects of refraction at intermediate frequencies (0.2 – 0.3 Hz). Both model runs clearly show the direction of the low frequency onshore propagating swell and the high frequency offshore travelling wind waves, as observed, but the region of the spectrum affected by refraction is not well modelled. The T&C source term apparently under-predicts the growth of waves at large angles to the wind and thus under-predicts the spectral levels of the refracted components below the peak frequency. On the other hand, the WAM-3 source term over-predicts this growth and therefore over-predicts the spectral energy. Directional spreading is not well modelled by either source term with WAM-3 over-predicting and T&C under-predicting the spread.

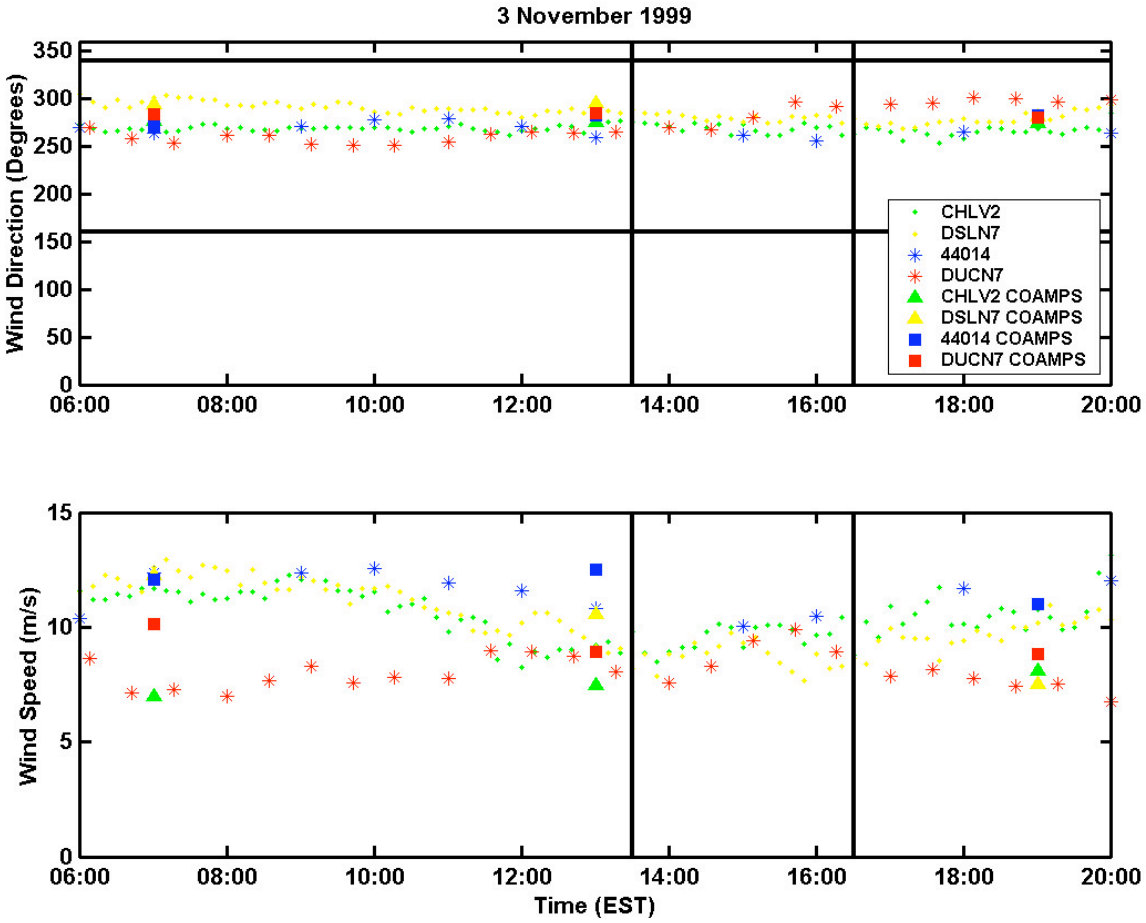

Figure 24. NDBC station wind speed and direction (from true north) observations over a fourteen-hour period on 3 November 1999 (SHOWEX, Case III) are compared with COAMPS model results. The black horizontal lines on the direction panel bracket the range for offshore winds and the black vertical lines indicate the selected time interval for Case III.

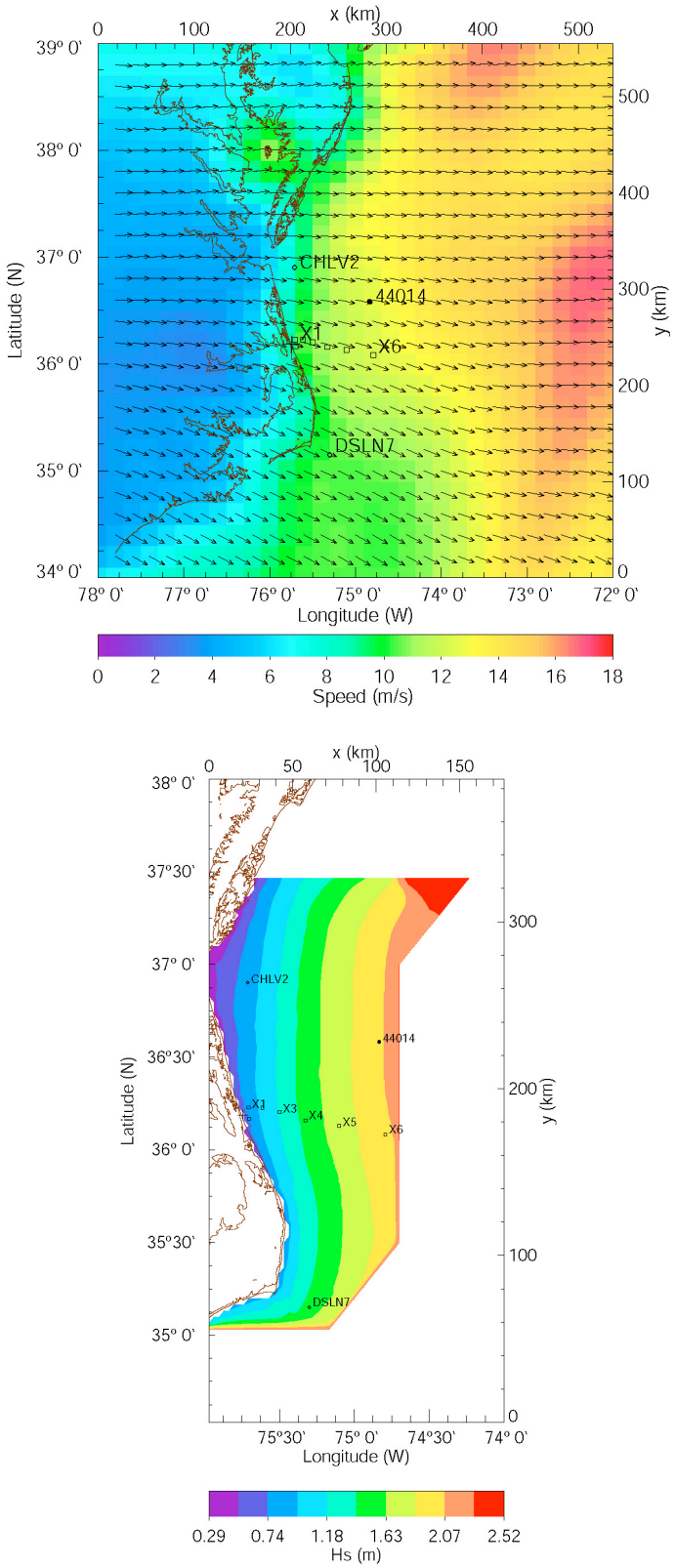

Figure 25. COAMPS wind speed and direction predictions at 1300 EST (Panel a) and WAVEWATCH III model domain with significant wave height predictions at 1700 EST (Panel b) on 3 November 1999 (courtesy of Dr Fabrice Ardhuin).

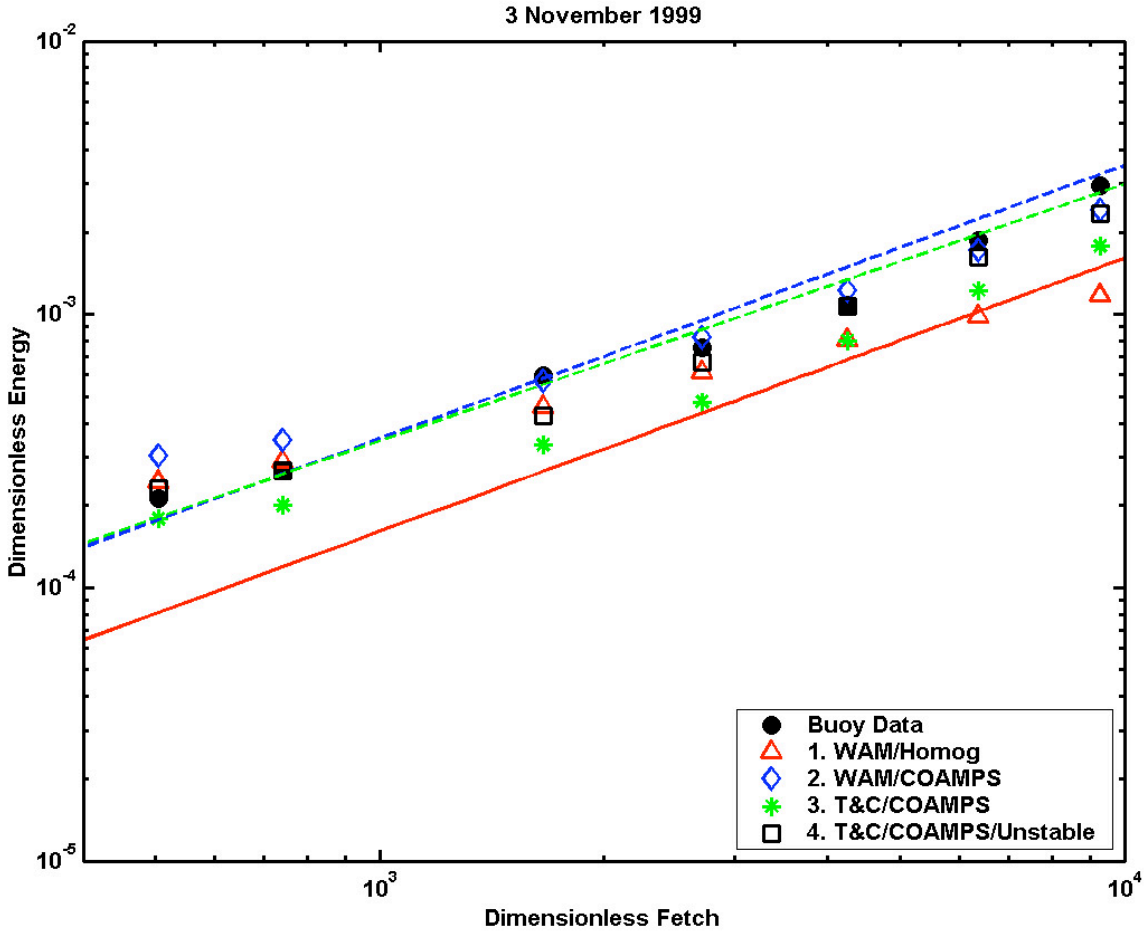

Figure 26. Growth of dimensionless energy as a function of dimensionless fetch for model Runs 1-4 (SHOWEX, Case III). The red line indicates the JONSWAP growth relation (Equation 9), the blue dashed line is Kahma's growth curve (Equation 11) and the green dashed line is the unstable growth relation of Kahma and Calkoen (Equation 15).

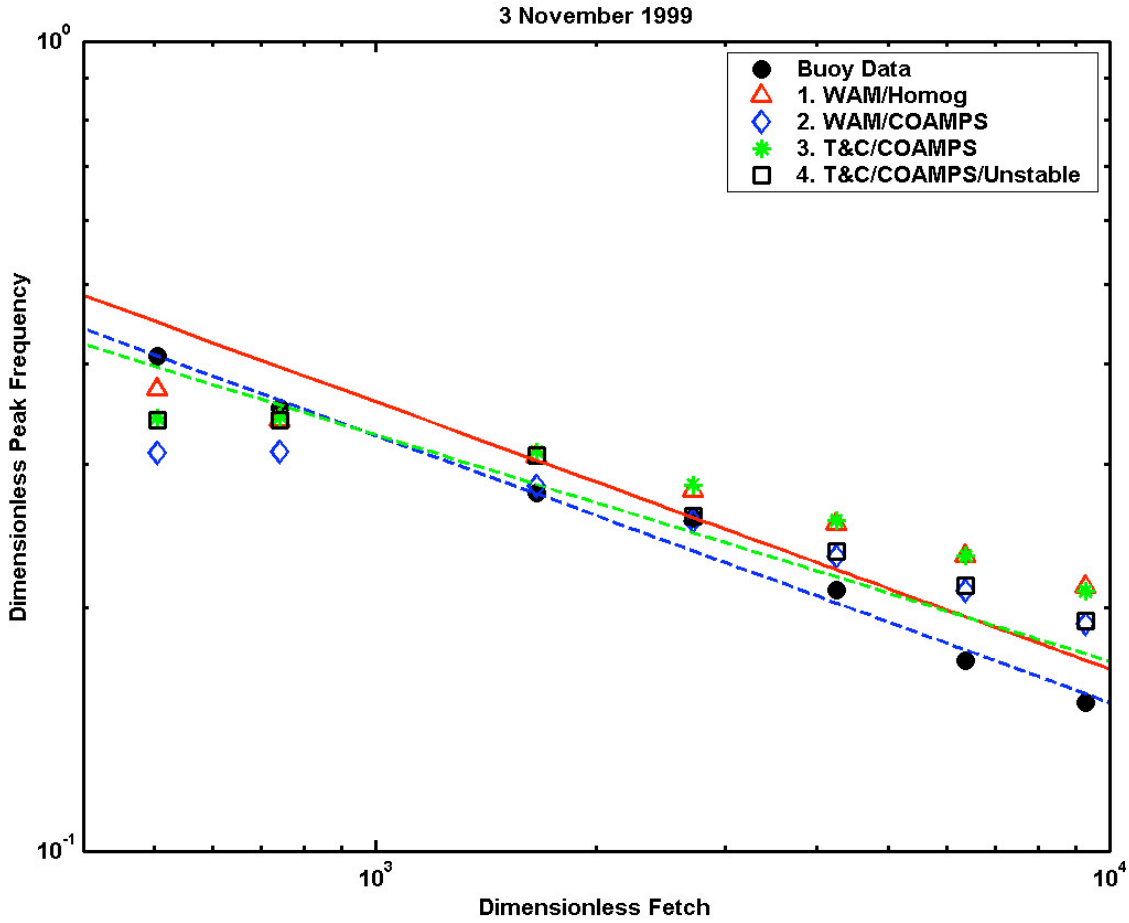

Figure 27. Growth of dimensionless peak frequency as a function of dimensionless fetch for model Runs 1-4 (SHOWEX, Case III). The red line indicates the JONSWAP growth relation (Equation 9), the blue dashed line is Kahma's growth curve (Equation 11) and the green dashed line is the unstable growth relation of Kahma and Calkoen (Equation 15).

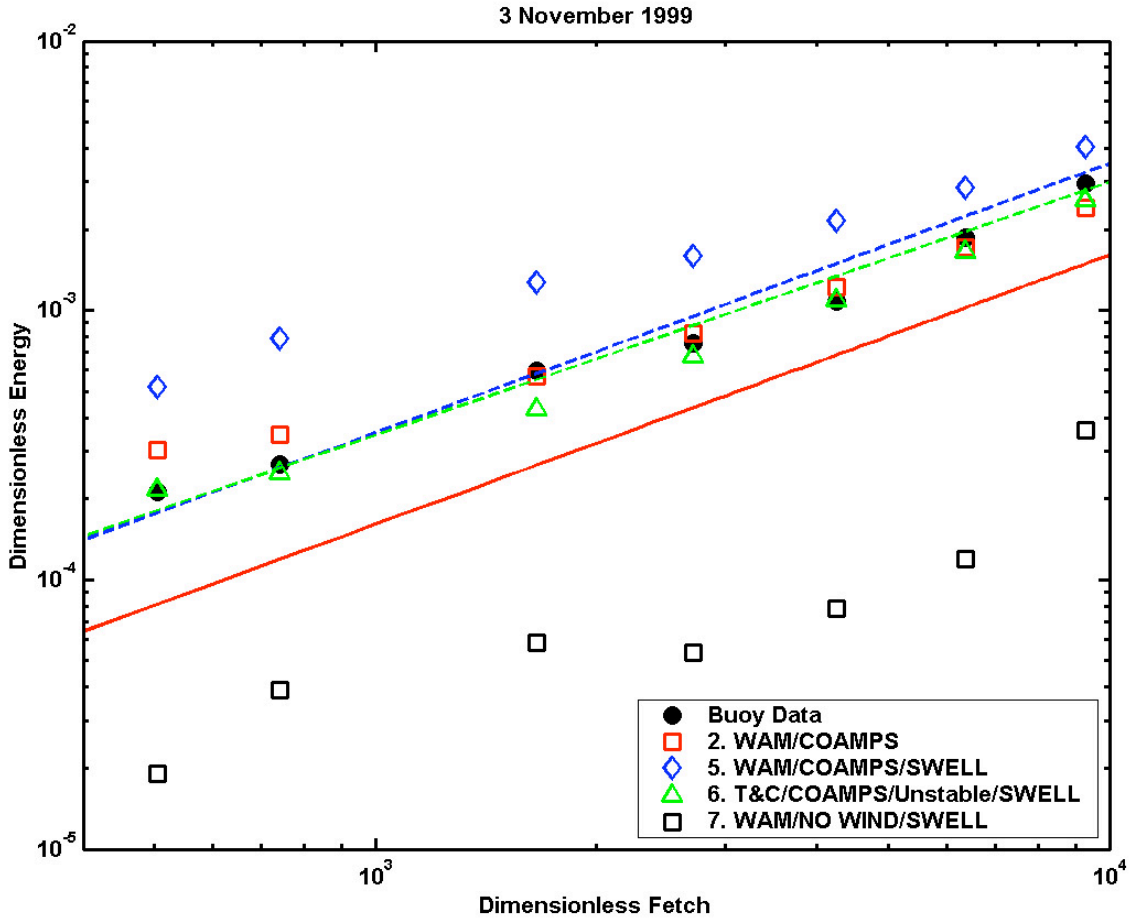

Figure 28. Growth of dimensionless energy as a function of dimensionless fetch for model Runs 2 and 5-7 (SHOWEX, Case III). Same format at Figure 26.

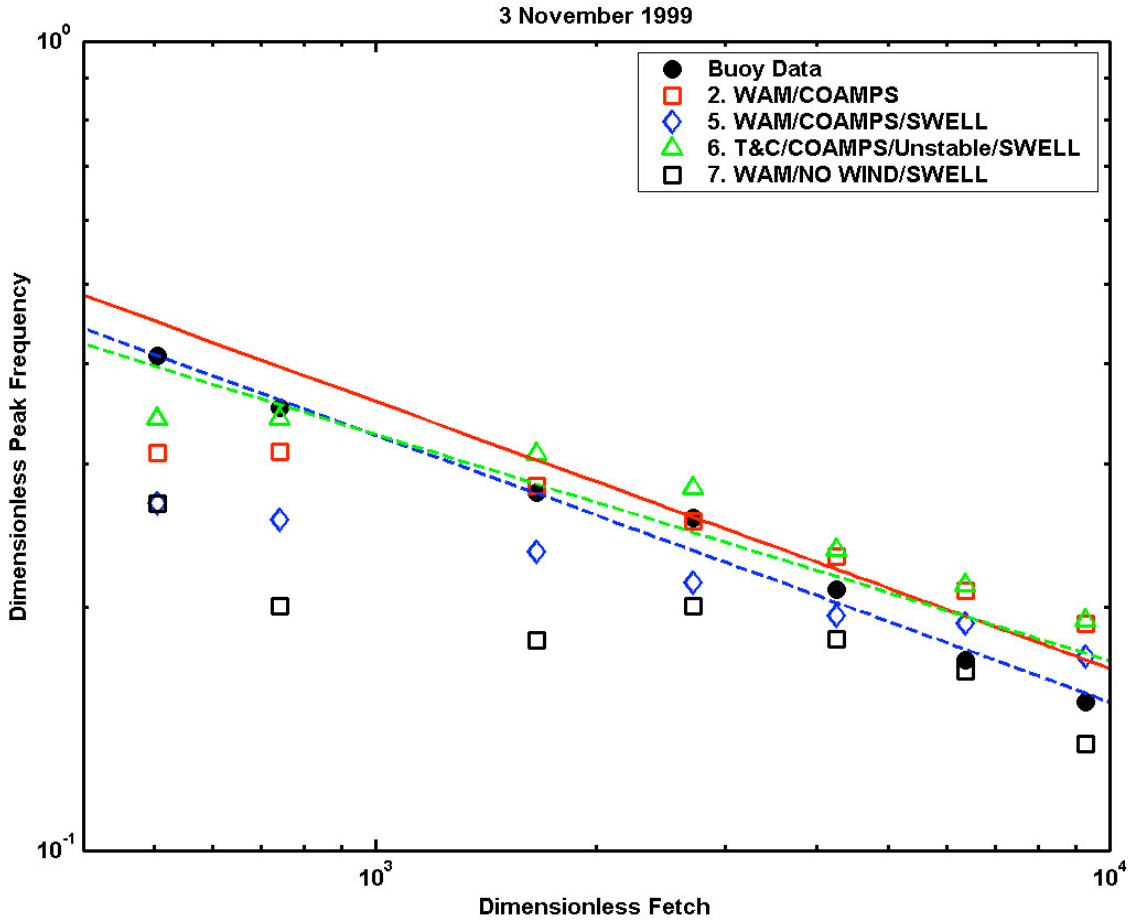

Figure 29. Growth of dimensionless peak frequency as a function of dimensionless fetch for model Runs 2 and 5-7 (SHOWEX, Case III). Same format as Figure 27.

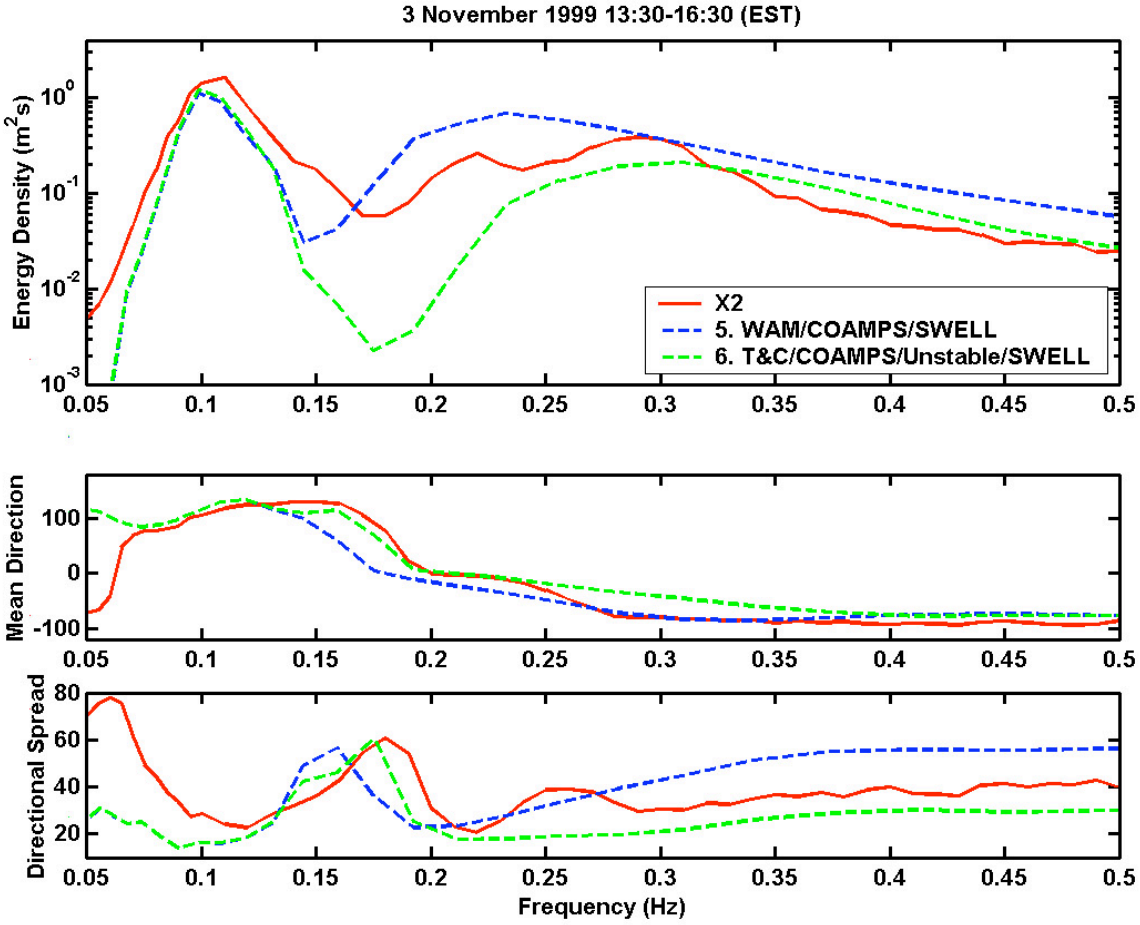

Figure 30. Energy density, mean wave direction and directional spreading as a function of frequency for buoy X2 and model Runs 5 and 6.

VI. CONCLUSIONS

Whilst much is known about the generation of wind waves in "ideal" conditions, natural conditions are often more complex in coastal environments. External influences such as the orientation of the wind with respect to the coastline, the bottom topography, atmospheric stability and the presence of swell, introduce considerable variability into the evolution of the wind wave field that is not well documented. The aim of this study was therefore to gain a greater understanding of fetch-limited wind wave generation on a natural continental shelf exposed to swell. This study was conducted over the North Carolina/Virginia continental shelf, off the east coast of the U.S. in the vicinity of Duck, North Carolina. Data were collected with a cross-shelf transect of six Datawell Directional Waverider buoys during the Shoaling Waves Experiment (1999) and two inner-shelf instrument arrays deployed during the SandyDuck Nearshore Field Experiment (1997). Additional wind and wave observations were obtained from permanent stations in the area, maintained by the U.S. Army Corps of Engineers Field Research Facility and the National Data Buoy Center.

Four case studies with steady offshore or alongshore winds (three from SHOWEX and one from SandyDuck) were selected for analysis of wind wave growth over the continental shelf. The observations revealed that the orientation of the mean wind direction, with respect to the coastline, was of critical importance in determining the evolution of the wind wave field, especially close to the coast. For the two cases with alongshore winds, wave properties were fairly uniform across the shelf, indicating that the waves were fully developed, except at locations close to the coast. Here, reduced energy levels were observed, a result of coastal sheltering and refraction effects. With alongshore winds, waves generated in the wind direction or on the offshore side of this direction experience an unlimited fetch and grow to full development. However, waves generated on the inshore side of the mean wind direction are severely fetch-limited, due to the close proximity of the coastline, and experience reduced growth. This asymmetrical fetch effect was most noticeable on the inner shelf where alongshore-

propagating wind waves were also affected by refraction over the shallow bathymetry and travelled along curved trajectories towards the coast.

One case with an almost shore-normal offshore wind represented nearly ideal fetch-limited conditions, but included energetic swell directionally opposing the wind seas. This case exhibited the classic fetch-limited spectral shape with pronounced overshoot of the wind wave peak levels, as observed during JONSWAP. Estimates of the Bulk Richardson Number indicated that the atmosphere was statically unstable. Consistent with this observation, the observed growth rates were closer to the growth curves proposed by Kahma (1981) for unstable atmospheric conditions, than the JONSWAP growth relations, which were calibrated for a stable atmosphere. The good agreement with Kahma's growth curves indicates that the presence of swell does not significantly affect the evolution of the wind wave field. The effects of coastal sheltering on directional wave properties were more severe in this case, compared with the alongshore wind cases, which was evident from the large shift in mean wave directions at low frequencies. Since the offshore wind had a small downcoast component, the resulting offshore travelling waves experience the combined effects of refraction and fetch asymmetry. As a result, the lower frequency waves travel preferentially downcoast at large angles to the wind.

One case with spatially varying winds exhibited the effects of non-local wind wave generation on the shelf. Wind waves forced by strong fetch-limited winds a few hundred kilometres to the south of the experiment site, were shown to undergo severe refraction over the shallow bathymetry. This resulted in a trapping of the waves along the shelf and a complete turning towards onshore arrivals at the instrument arrays.

One offshore wind case was selected for further examination and comparison with model results. A series of runs, with and without swell, were conducted using the WAVEWATCH III third generation model, forced with COAMPS winds, using two different source term formulations. The widely used WAM cycle 3 parameterisation and the more recent source term proposed by Tolman and Chalikov (1996) only differ in their wind input and dissipation formulations. Comparisons with observations highlight some of the known shortcomings of the WAM-3 source terms, that is, a flattening out of the

growth curves compared with the JONSWAP relationship and spurious growth of wind waves in the presence of swell. Overall, better agreement with the observations was found by using the Tolman and Chalikov source term, but this formulation tends to under-predict the growth of waves at large angles relative to the wind.

THIS PAGE INTENTIONALLY LEFT BLANK

LIST OF REFERENCES

Ardhuin, F., O'Reilly, W.C., Herbers, T.H.C., and Jessen, P.F., "Swell transformation across the continental shelf. Part I: Attenuation and directional broadening." *Journal of Physical Oceanography,* v. 33, pp. 1921-1939, 2003.

Booij, N., Ris, R.C. and Holthuijsen, L.H., "A third-generation wave model for coastal regions." *Journal of Geophysical Research,* v. 104, No. C4, pp 7649-7666, April 1999.

Borbash, M. I., "Observed directional spectra of shoaling and breaking waves." Master's Thesis, Naval Postgraduate School, Monterey, California, June 1998.

Charnock, H., "Wind stress on a water surface." *Quarterly Journal of the Royal Meteorological Society*, v. 81, pp. 639-640, 1955.

Donelan, M.A., Hamilton, J. and Hui, W.H., "Directional spectra of wind-generated waves." *Phil. Trans. R. Soc. Lond.* v. A 315, pp. 509-562, 1985.

Hasselmann, K. et al., "Measurements of wind-wave growth and swell decay during the Joint North Sea Wave Project (JONSWAP)." *Dtsch. Hydrogr. Z.,* A8, No. 12, 95 pp., 1973.

Hasselmann, S., and Hasselmann, K., "Computations and parameterisations of the nonlinear energy transfer in a gravity-wave spectrum. Part I: A new method for efficient computations of the exact nonlinear transfer integral." *Journal of Physical Oceanography,* v. 15, pp. 1369-1377, 1985.

Herbers, T.H.C., Hendrickson, E.J. and O'Reilly, W.C., "Propagation of swell across a wide continental shelf." *Journal of Geophysical Research,* v. 105, No. C8, pp. 19,729-19,737, August 2000.

Holthuijsen, L.H., Ris, R.C., Booij, N. and Cecchi, E., "Swell and whitecapping, a numerical experiment." *7th Int. Conf. Coastal Engng.,* Sydney, p. 346-344, 2000.

Kahma, K.K., "A study of the growth of the wave spectrum with fetch." *Journal of Physical Oceanography,* v. 11, pp. 1503-1515, November 1981.

Kahma, K.K., and Calkoen, C.J., "Reconciling discrepancies in the observed growth of wind-generated waves." *Journal of Physical Oceanography,* v. 22, pp. 1389-1405, December 1992.

Kitaigorodskii, S.A., "Application of the theory of similarity to the analysis of wind-generated water waves as a stochastic process." *Bull. Acad. Sci. USSR Geophys.,* Ser. No.1, 73p, 1962.

Kitaigorodskii, S.A., "On the theory of the equilibrium range in the spectrum of wind-generated gravity waves." *Journal of Physical Oceanography,* v. 13, pp. 816-827, 1983.

Komen, G.J., Hasselmann, S. and Hasselmann, K., "On the existence of a fully developed wind-sea spectrum." *Journal of Physical Oceanography,* v. 14, pp. 1271-1285, August 1984.

Komen, G.J., Cavaleri, L., Donelan, M., Hasselmann, K., Hasselmann, S., and Janssen, P.A.E.M., *Dynamics and Modelling of Ocean Waves*. Cambridge University Press, 1994.

Lygre, A., and Krogstad, H.E., "Maximum entropy estimation of the directional distribution in ocean wave spectra." *Journal of Physical Oceanography,* v.16, pp. 2052-2060, 1986.

National Ocean Service, U.S. Department of Commerce, National Oceanic and Atmospheric Administration, *United States Coast Pilot Volume 4: Cape Henry to Key West,* pp. 188-191 & 198, Government Printing Office, Washington D.C., July 2002.

Pierson, W.J., Jr. and Moskowitz, L., "A proposed spectral form for fully developed wind seas based on the similarity theory of S.A. Kitaigorodskii." *Journal of Geophysical Research,* v. 69, p. 5181, 1964.

Phillips, O.M., "The equilibrium range in the spectrum of wind-generated water waves." *Journal of Fluid Mechanics,* v. 4, pp. 426-434, 1958.

Snyder, R.L., Dobson, F.W., Elliott, J.A., and Long, R.B., "Array measurements of atmospheric pressure fluctuations above surface gravity waves." *Journal of Fluid Mechanics,* v. 102, pp. 1-59, 1981.

Stull, R.B., *An Introduction to Boundary Layer Meteorology*, pp. 376-381, Kluwer Academic Publishers, 1988.

Tolman, H.L., "A third-generation model for wind waves on slowly varying, unsteady, and inhomogeneous depths and currents." *Journal of Physical Oceanography,* v.21, pp.782-797, June 1991.

Tolman, H.L., "User manual and system documentation of WAVEWATCH-III version 2.22." *WAVEWATCH III,* U.S. Department of Commerce, National Oceanic and Atmospheric Administration, National Weather Service, Technical Note, September 2002. [www.polar.wwb.noaa.gov/waves/wavewatch/wavewatch.html]

Tolman, H.L., *WAVEWATCH III*, U.S. Department of Commerce, National Oceanic and Atmospheric Administration, National Weather Service, [www.polar.wwb.noaa.gov/waves/wavewatch/wavewatch.html], September 2003.

Tolman, H.L. and Chalikov, D.V., "Source terms in a third-generation wind-wave model." *Journal of Physical Oceanography,* v. 26. pp. 2497-2518, November 1996.

WAMDI Group, "The WAM model – A third generation ocean wave prediction model. "*Journal of Physical Oceanography,* v. 18, pp. 1775-1810, December 1988.

Wang, D.W. and Hwang, P.A., "Evolution of the bimodal directional distribution of ocean waves." *Journal of Physical Oceanography,* v. 31, pp. 1200-1221, May 2001.

Walsh, E.J., Hancock, D.W., Hines, D.E., Swift, R.N., and Scott, J.F., "An observation of the directional wave spectrum evolution from shoreline to fully developed." *Journal of Physical Oceanography,* v. 19, pp. 670-690, May 1989.

Young, I.R and Verhagen, L.A., "A note on the bimodal directional spreading of fetch-limited wind waves." *Journal of Geophysical Research,* v. 100, No. C1, pp. 773-778, January 1995.

Young, I.R, Verhagen, L.A. and Banner, M.L., "The growth of fetch limited waves in water of finite depth. Part 1. Total energy and peak frequency." *Coastal Engineering*, v. 29, pp. 47-78, 1996.

THIS PAGE INTENTIONALLY LEFT BLANK

INITIAL DISTRIBUTION LIST

1. Defense Technical Information Center
   Ft. Belvoir, Virginia

2. Dudley Knox Library
   Naval Postgraduate School
   Monterey, California

3. Professor Mary L. Batteen, Department of Oceanography (Code OC/Bv)
   Naval Postgraduate School
   Monterey, California

4. Professor Thomas H.C. Herbers, Department of Oceanography (Code OC/He)
   Naval Postgraduate School
   Monterey, California

5. Professor Edward B. Thornton, Department of Oceanography (Code OC/Tm)
   Naval Postgraduate School
   Monterey, California

6. Dr Fabrice Ardhuin
   Service Hydrographique et Oc'eanographique de la Marine
   Brest, France

7. Mr Paul Jessen, Department of Oceanography
   Naval Postgraduate School
   Monterey, California

8. LCDR Andrew McCrindell
   Directorate of Oceanography and Meteorology
   Sydney, NSW, Australia

9. LEUT Kristen Watts
   Directorate of Oceanography and Meteorology
   Sydney, NSW, Australia